PERGAMON

Journal of Structural Geology 24 (2002) 1–24

JOURNAL OF STRUCTURAL GEOLOGY

www.elsevier.com/locate/jstrugeo

Palaeoproterozoic regional-scale non-coaxial deformation: an example from eastern Eyre Peninsula, South Australia

J.J. Vassallo, C.J.L. Wilson*

School of Earth Sciences, The University of Melbourne, Victoria 3010, Australia

Received 15 December 1999; revised 25 February 2001; accepted 16 March 2001

Abstract

Regional-scale high-grade structures preserved in an Archaean–Palaeoproterozoic gneissic belt, in eastern Eyre Peninsula, are attributed to the development of the Kalinjala Shear Zone. The Kalinjala Shear Zone is an ~200 km long high-grade dextral transpressional shear zone that formed during the ~1730–1700 Ma Kimban Orogeny (KD_1 and KD_2). The first deformation event, KD_1, involved a large component of northeast–southwest sub-horizontal stretching (parallel to X) and formed abundant meso- to macro-scale sheath folds and a well-developed prolate >10:1:1 ($X > Y > Z$) L-fabric (KL_1; $L \gg S$) during transitional granulite facies conditions. The second event, KD_2, was dominated by bulk sub-horizontal flattening along the east–west Z-axis following KD_1. KD_2 formed variably-dipping and mutually overprinting reverse and strike–slip shear zones, upright, tight-isoclinal folds and plane strain ~12:3:1 marker clasts. The strain studies indicate the primary role of constrictional strains during the transpressional deformation and the smaller degree of flattening recorded in the amphibolite to granulite facies shear belt. The size of this Proterozoic shear belt is akin to those of modern orogens involved in significant plate reorganisation.

Keywords: Deformation; Kalinjala Shear Zone; Paleoproterozoic; South Australia; Strain

1. Introduction

Regional-scale shear zones are prevalent in terrains of Archaean to Phanerozoic in age. Shear systems, over time, do not appear to have changed the way they have developed micro- and meso-structurally, implying distinct similarities also in macrostructural processes (Windley, 1993). One feature particularly worthy of note is the size of these systems determined by the amount of strike–slip displacement. Many deep crustal structures that are associated with significant tectonic plate reorganisations have offsets of several hundred kilometres (Median Tectonic Line, southwest Japan; Brown, 1998). It would be expected that portions of these ancient crustal structures would be preserved, due to their extensive strike lengths. However, this is commonly not the case, and only small sections or the margins of these shear zones remain, leaving highly deformed belts that are somewhat enigmatic in origin. Therefore, the increasing identification of ancient regional structures and their kinematics in areas of limited outcrops is of great interest as they may lead to mountain belt and plate reconstructions.

Coaxial vs non-coaxial deformation and their recognition on a regional scale in any deformed terrain are critical when reconstructing the tectonic history of an orogenic belt. This is pivotal when inferring an overall direction of tectonic transport in high-grade metamorphic terrains where grain growth may obliterate any pre-existing fabrics. If a coaxial model is invoked for an area that has undergone a non-coaxial deformation the implied direction of transport could be perpendicular to the true direction of transport. In some orogens this distinction may be determined with relative ease if significant proportions of the belt are exposed. However, in areas of poor exposure, like Eyre Peninsula in South Australia (Fig. 1), this differentiation is very difficult. The presence of large ductile shear zones in this terrain can only be inferred by analysing meso-scale structures in conjunction with the use of geophysical mapping techniques.

Highly non-cylindrical folds or sheath/tubular folds are characteristic of many ductile shear zones (Cobbold and Quinquis, 1980; Ghosh, 1993; Alsop and Holdsworth, 1999). However, they may be easily overlooked especially if they formed early during the deformation history and were subsequently deformed. Good indicators that a belt contains sheath folds (and therefore has been deformed by non-coaxial processes) include: (i) early penetrative

* Corresponding author. Tel.: +61-3-8344-6538; fax: +61-3-8344-7761.
E-mail address: cjlw@unimelb.edu.au (C.J.L. Wilson).

0191-8141/02/$ - see front matter
PII: S0191-8141(01)00043-8

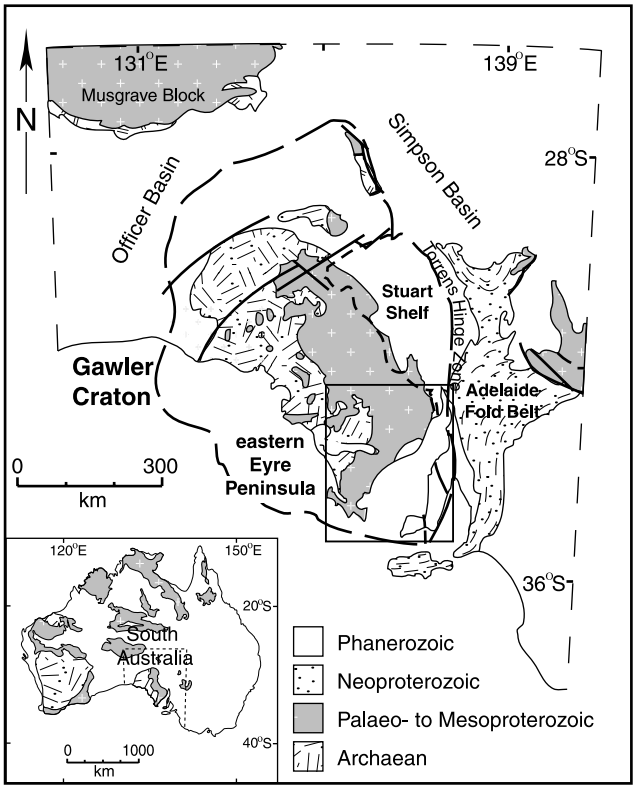

Fig. 1. The regional geology of South Australia highlighting the position of the Gawler Craton. Inset shows the location of the eastern Eyre Peninsula (see Fig. 2).

layer-parallel high-strain fabrics; (ii) extensive areas containing highly prolate clasts (the rocks are *L*-tectonites); (iii) the presence of both Type 2 and Type 3 interference patterns with an elongation lineation parallel to the fold hinge lines; (iv) many overturned units (Cobbold and Quinquis, 1980; Skjernaa, 1989).

In this paper we describe the mesoscopic structural features of some reworked Archaean and Proterozoic gneisses that attained amphibolite and granulite facies metamorphic grades during the Palaeoproterozoic. We relate these mesoscopic structures to regional strain patterns highlighted by aeromagnetic signatures in order to determine the regional-scale structure associated with a continental-scale shear zone and discuss its greater significance.

2. Regional geology of the eastern Gawler Craton

Eastern Eyre Peninsula comprises two high-grade Archaean–Palaeoproterozoic metamorphic terrains believed to be juxtaposed by a >200 km long sigmoidal reactivated high-grade shear zone, previously referred to as the Kalinjala Mylonite Zone (Parker, 1980). However, we will refer to this high-strain zone as the Kalinjala Shear Zone because it is a composite high-strain zone that includes a variety of fault rock types that are not exclusively mylonites. Well-exposed coastal platforms in southeastern Eyre Peninsula provide strike–normal and strike–parallel sections across the southern portion of the terrain (Figs. 2 and 3). Successively older rocks are encountered from east to west, implying that either a vertical crustal section is traversed across this zone, or two distinct crustal blocks have been amalgamated.

Five tectonic events are thought to have affected this belt (Fig. 4). These are: (1) the 2400 Ma Sleafordian Orogeny (Fanning et al., 1980a); (2) the 2000 Ma Miltalie Event (Parker, 1993); (3) the 1850 Ma Lincoln Orogeny (Vassallo and Wilson, 1999a,b); (4) the ~1700 Ma Kimban Orogeny (Parker and Lemon, 1982); and (5) the 1500 Ma Wartakan Event (Parker, 1993). However, the Kimban Orogeny has all but obliterated products of the three earlier events. Structurally, there is no evidence for the existence of the Sleafordian Orogeny at its type area (Whalers Way: Fig. 3). Metamorphic zircons have been extracted from the Sleaford Complex suggesting that high temperatures were achieved around 2400 Ma, but any related structures in the study areas described here have been completely transposed by Kimban structures. No structures have been convincingly reported to relate to the Miltalie Event. In areas of Kimban low-strain the effects of the Lincoln Orogeny are also low-strain, suggesting that it was not an extensively intense event. The Wartakan event has only produced localised high-strain structures that are easily distinguishable from the Kimban as they contain fine-grained muscovite-bearing fabrics that overgrow high-grade Kimban fabrics. Therefore, the gross physical architecture and high-strain structures of the Kimban Orogeny have remained relatively unchanged since they were formed and structures related to prior deformations appear to have either been weak, or unknown.

2.1. Archaean gneisses and deformation

The Archaean Sleaford Complex (Fig. 3) is the oldest crystalline basement sequence and only crops out west of the Kalinjala Shear Zone. It consists of three units: (1) the >2600 Ma Carnot Gneisses (Fanning, 1997), a series of highly deformed high-grade layered paragneisses and mafic gneisses, and syn-orogenic intrusives (Fanning et al., 1988); (2) the weakly-deformed ~2460–2520 Ma (Fanning, 1997) syn-tectonic Dutton Suite intrusives; and (3) the moderately-deformed amphibolite facies 2479 ± 8 Ma Wangary Gneiss (Fanning et al., 1980a,b; Parker et al., 1988; Fanning, 1997). Zircons recovered from Carnot Gneiss pelitic units suggest ~3000 Ma inheritance and that peak metamorphic conditions were attained at ~2420 Ma (U–Pb monazite SHRIMP; Fanning, 1997; Fanning and Aleinikoff, 1998). Therefore, sedimentary deposition and magmatic intrusion must have ceased during the Late Archaean–Early Proterozoic.

2.2. Palaeoproterozoic gneisses and deformation

Zircon growth at 2003 ± 13 Ma in the orthogneissic

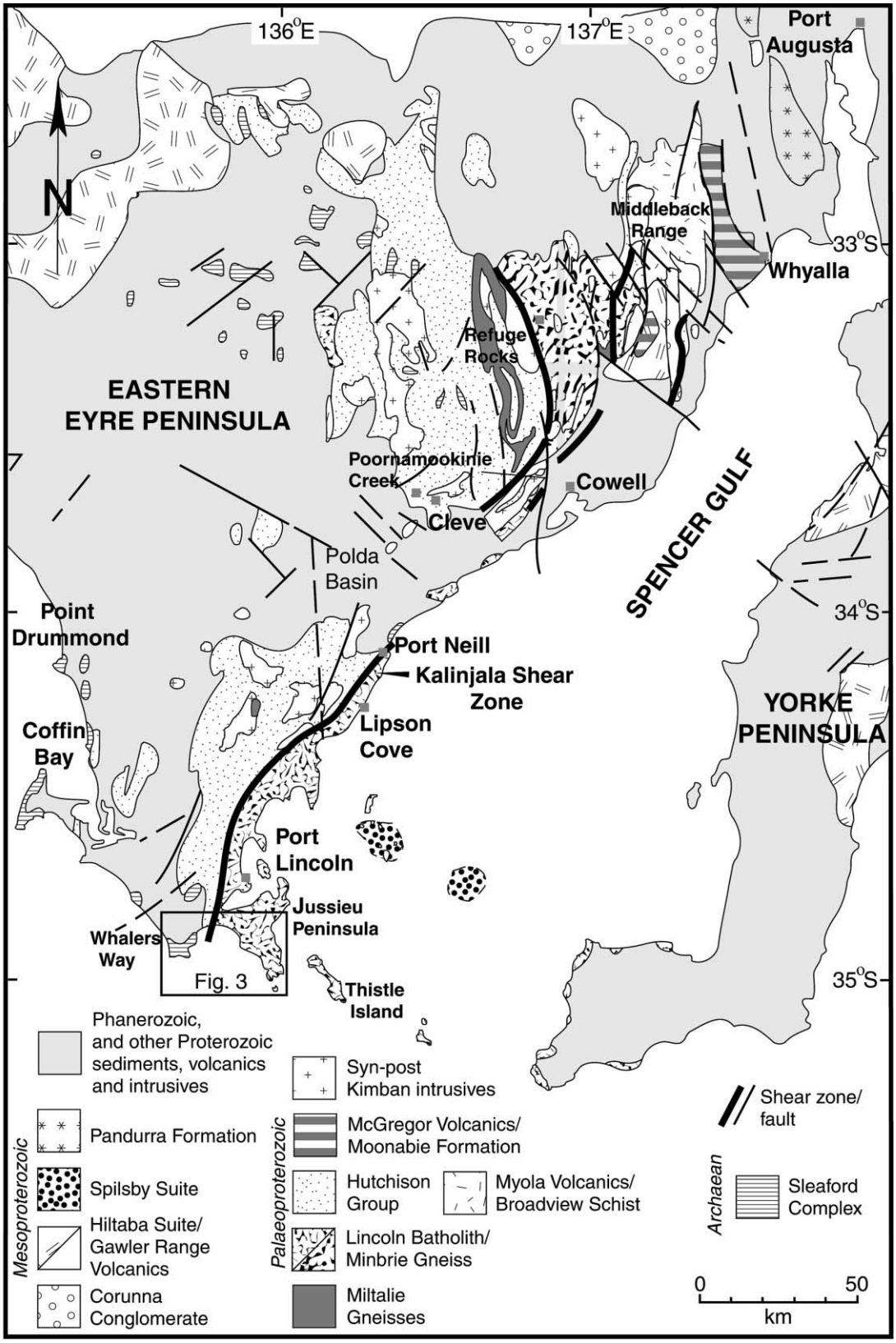

Fig. 2. Geology of eastern Eyre Peninsula and outline of the main structural elements of the region after Drexel et al. (1993). Inset shows the location of Fig. 3.

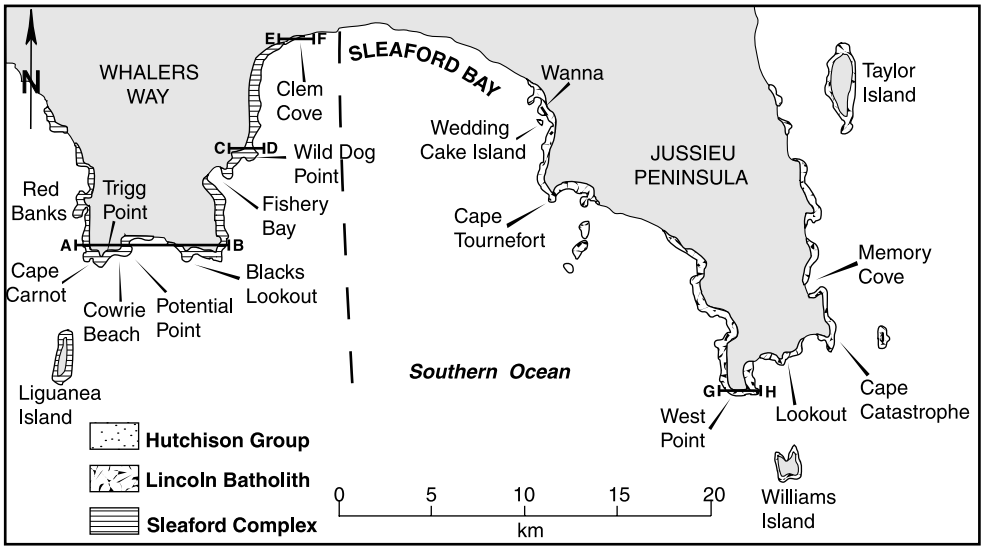

Fig. 3. Localities along the southern Eyre Peninsula coast. Dashed line is the position of the Kalinjala Shear Zone inferred from aeromagnetic images. Cross-section lines A-H refer to the four sections shown in Fig. 9.

Miltalie Gneiss (Fig. 4), and three other felsic gneisses of equivalent ages, represent the second known magmatic event recorded in Eyre Peninsula (Fanning, 1997). Rocks of this age crop out along the southwestern margin of the Kalinjala Shear Zone (Fig. 2). The high-grade metamorphic Miltalie Event (Fig. 4) is interpreted to have followed the intrusion of the Miltalie Gneiss at ~1964 Ma (Fanning et al., 1988).

2.3. The Lincoln Batholith

The ~1850 Ma Lincoln Batholith represents a large addition of relatively anhydrous 'I-type' melts into the mid- to lower-crust (>8 kbar and 845°C) and is the third major magmatic period in the region (Figs. 2 and 3; Mortimer et al., 1988; Fanning, 1997). The batholith is charnockitic and consists of foliated mafic-felsic pyroxene- to hornblende–biotite-bearing megacrystic and even-grained gneisses (Fanning et al., 1988; Schaefer, 1998). A suite of deformed hornblende-bearing granodiorites and augen gneisses metamorphosed to amphibolite facies (Minbrie Gneisses) in the Refuge Rocks area are interpreted to be mid-crustal equivalents of the Lincoln Batholith (Drexel et al., 1993). Vassallo and Wilson (1999b) distinguished two deformational events (LD_1 and LD_2—prefixes *L*, *K* or *Sl* refer to Lincoln, Kimban and Sleafordian orogenies, respectively) in the Lincoln Batholith (Fig. 4) that they interpreted to have occurred prior to intrusion of a series of straight-sided mafic dykes, the Tournefort dykes (Parker et al., 1987). Northerly-plunging upright folds, sub-vertical shear zones and boudins with north-striking axes characterise these events and suggest they formed during an east–west compressional phase associated with the intrusion of the batholith.

2.4. The Hutchison Group

The Hutchison Group is inferred to be a series of deformed and metamorphosed shallow to deep marine sediments (Parker and Lemon, 1982; Rankin et al., 1988; Drexel et al., 1993). The Hutchison Group marks the most significant depositional event in the early Proterozoic. Parker and Lemon (1982), reconstructed the stratigraphy which included the occurrence of two identical Jaspilite units, specifically used as separate stratigraphic marker horizons. However, Vassallo and Wilson (2001) have reinterpreted the sequence and suggested that the stratigraphy is simpler than suggested by Parker and Lemon (1982), as there is only one Jaspilite unit that has been repeated by folds and thrusts. On this basis, deposition is believed to have begun as a fluvial or shallow-marine clastic wedge with basal conglomeratic feldspathic quartzites resting unconformably on Miltalie Gneiss basement. These sediments were followed by the deposition of massive to poorly-layered medium-grained dolomitic marbles. The marbles were overlain by the Middleback Jaspilite (composed of magnetite quartzites, schists and dark-coloured cherts). The ~500 m thick Cook Gap Schist (correlated with the Mangalo Schist), that consists of garnet–mica schists, calc–silicate gneiss and concordant amphibolite, overlies the Jaspilite units. Pelitic to semi-pelitic schist and metasiltstone, as well as interlayered diopside-rich calc–silicates and felsic gneisses (Bosanquet formation) form the Upper Hutchison Group (Drexel et al., 1993).

Vassallo and Wilson (2001) argued that the Hutchison Group may be ~1800 Ma. That is, the Lincoln Batholith is basement to these metasediments and that they were deposited synchronously with intrusion of the Tournefort dykes (Section 2.5). This interpretation is in disagreement

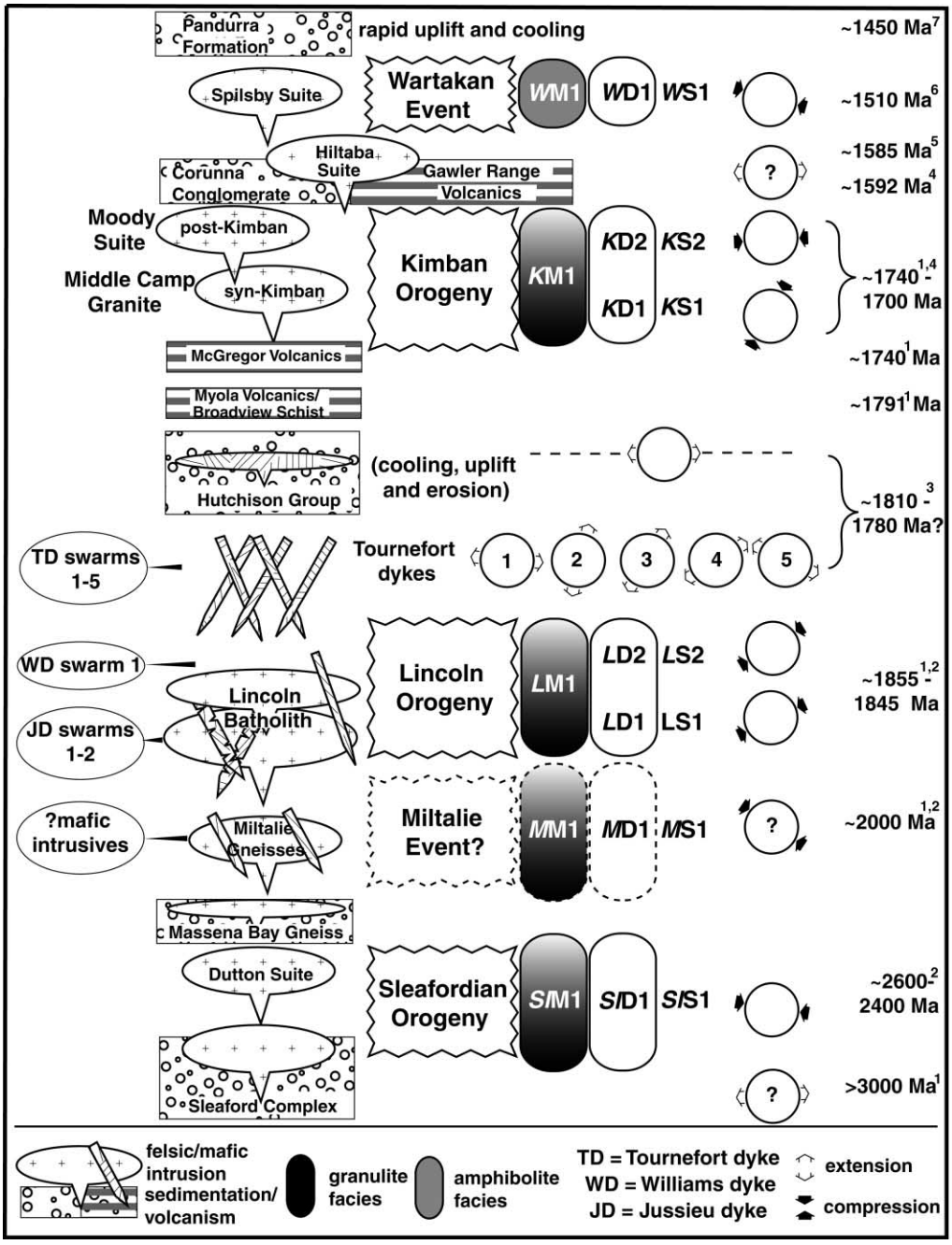

Fig. 4. Archaean to Mesoproterozoic evolution of eastern Eyre Peninsula. References of age dates refer to: (1) Fanning (1997); (2) Webb et al. (1986) and Fanning et al. (1988); (3) Schaefer (1998); (4) Drexel et al. (1993); (5) Creaser and Fanning (1993); (6) Fanning (1997) and (7) Foster and Ehlers (1998).

with earlier suggestions that the Hutchison Group was deposited between the periods ~1964–1850 Ma (Parker, 1993).

2.5. Tournefort dykes

The abundant, straight-sided, mafic, continental tholeiitic 1812 ± 5 Ma Tournefort dykes crosscut the Lincoln Batholith (Drexel et al., 1993; Schaefer, 1998). In low-strain zones original en échelon emplacement fractures are preserved indicating emplacement occurred as a result of tensional stresses (e.g. Pollard et al., 1982). Hoek and Schaefer (1998) suggested that the dykes are the products of a widespread extensional event. In this study, five generations of Tournefort dyke have been identified (TD_1–TD_5) on the basis of mutual crosscutting relationships in weakly deformed areas (Fig. 5).

The label 'Tournefort dyke' so far has only been restricted to those mafic dykes that intruded the Lincoln Batholith. However, multitudes of deformed and metamorphosed post-Miltalie Gneiss mafic dykes crop out along the Whalers Way coast (Fig. 3) that are texturally

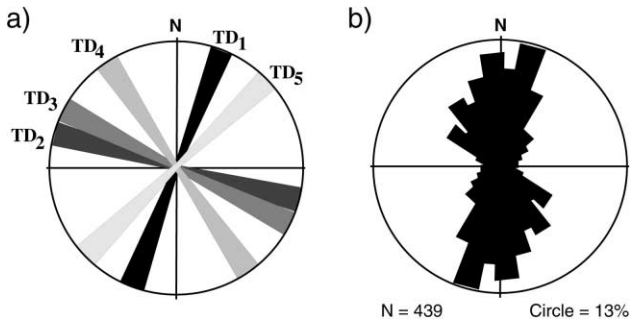

Fig. 5. Orientations of the Tournefort dykes in the Lincoln Batholith (a) Orientations of five generations of Tournefort dykes (TD_{1-5}) based on mutual crosscutting relationships in areas of low-strain. (b) Orientations of deformed and undeformed dykes from all five groups collected from Jussieu Peninsula. The greater trend to the N suggests N–S stretching of the block.

identical and chemically inseparable from the Tournefort dykes. Schaefer (1998) used the Nd-isotopic ratios and chemical evidence of Turner et al. (1993) to determine that a mafic dyke transecting the Sleaford Complex in Fishery Bay is 'isotopically indistinguishable from the Tournefort dykes'. Therefore, those post-Miltalie Gneiss mafic dykes that crop out at Whalers Way are referred to as Tournefort dykes herein.

2.6. Syn- to post-Kimban intrusives

Various syn-Kimban granitic rocks have intruded the older sequences and were deformed with them. One pluton most worthy of note is the Middle-Camp granite (~1730 Ma; Schwarz unpublished SHRIMP U–Pb data) which lies in the northern bifurcation of the Kalinjala Shear Zone (Fig. 1).

Granites and adamellites of the post-Kimban ~1700 Ma Moody Granitoid Suite represent the fifth magmatic period preserved in the belt (Fig. 4). Pluton-sized bodies of this age have only been recognised in the Hutchison Group. The plutons are variably foliated and contain hornblende and biotite, with or without garnet. The 1702 ± 10 Ma Chinmina Syenite is the youngest unit in this suite (Fanning, 1997). Weakly deformed felsic dykes in the Lincoln Batholith and Sleaford Complex may also belong to this suite.

2.7. Mesoproterozoic rocks and deformation

Mesoproterozoic sedimentary deposition and magmatic intrusions reflect the last mobile stages of the belt (Drexel et al., 1993; Foster and Ehlers, 1998). Deformation during the Mesoproterozoic formed cross-folds, fracture zones and northwest-trending lineaments collectively labelled as the ~1510 Ma Wartakan Event (WD_1) (Fanning et al., 1988). Deposition of arenaceous redbeds of the Pandurra Formation in an apparent graben accompanied rapid regional uplift marking cratonisation of the Gawler Craton (Parker, 1993).

3. Reinterpretation of the Kimban Orogeny

The beginning and end of the Kimban Orogeny are marked by two separate magmatic episodes. The ~1810 Ma Tournefort dykes (Schaefer, 1998) intruded before deformation was initiated and provide a lower limit for its commencement. An upper limit for the Kimban tectonic activity is provided by undeformed post-Kimban ~1700 Ma Moody Granitoid Suite felsic intrusives (Schwarz, 1999). Whole-rock Sm–Nd analyses of garnet–hornblende high-strain fabrics in deformed Tournefort dykes suggest that peak conditions were achieved at $\sim 1730 \pm 20$ Ma (Hand et al., 1995). Argon–Argon dating of single metamorphic hornblende and biotite grains indicate that post-peak thermal conditions outlived deformation by 100 million years until ~1600 Ma (Foster and Ehlers, 1998).

We recognise two main styles of structural development (KD_1–KD_2) across the belt, an interpretation which significantly differs from those presented by previous workers as

Fig. 6. Photographs of representative structures formed during the Kimban Orogeny. (a) A vertical section perpendicular to the long axis of a mesoscopic sheath fold in Sleaford Complex metapelitic and mafic units at Fishery Bay. Note the double fold closure in the centre of the photograph highlighting the asymmetry of the fold in three dimensions. KS_1 is parallel to the layering and has a low ellipticity suggesting the rocks have not been significantly flattened in this area. Looking north; pencil points east. (b) Section through a sheath fold that has a 'boomerang-shaped' outline in Hutchison Group metasediments at Clem Cove, Sleaford Bay. The axis of the fold has been rotated to the east by dextral reverse shears (see Fig. 9) causing KS_2 to dip ~45° to the west. Ruler is parallel to KS_2. cs = calc-silicate gneiss; gs = graphitic schist. (c) A strongly flattened mesoscopic sheath fold in highly-strained felsic and mafic gneisses at Black's Lookout. The flattening produced upright disharmonic chevron folds with fold axes sub-parallel to the gentle southerly-plunging KL_1. (d) Linked mesoscopic shear zones in a north-facing section that dissect pre-existing sheath folds at Fishery Bay. The shears indicate predominant west-block up reverse movement and transect KS_1 and a parallel generation of leucosomes in metapelitic units of the Sleaford Complex. KD_2 leucosomes are localised in the shears. Looking north. (a)–(d) show the structures believed to form as a result of progressive flattening of the sheath folds to until they are no longer recognisable as such. (e) A mafic dyke in highly-strained felsic gneisses showing an example of symmetrical boudinage. The dyke fragments have 'fish-mouthed' neck shapes suggesting the mafic units were more competent during their development. The high-grade nature of the deformation is shown by the development of coarse-grained quartz–feldspar–biotite pegmatitic leucosomes in the boudin necks (arrow). The leucosomes commonly retain igneous textures suggesting that they formed in the latter stages of KD_2. Ruler points north. (f) A high-grade shear zone on the eastern side of Williams Island. Strain is focussed in 11 amalgamated Tournefort dykes that are surrounded by low-strain metagranitoids. Boudinage structures suggest that north–south elongation followed the primary development of the shear zone. Ruler points north. (g) A section parallel to KS_2 through a KD_2 shear zone in a Lincoln Batholith metagranitoid at Lookout. The strong prolate shape of the steeply south-plunging clasts record the imposition of intense constrictional strains. (h) $S \wedge C$ fabrics in a sheared Lincoln Batholith megacrystic metagranitoid. The granulation of the former rectangular feldspar porphyroclasts indicates high strain. Ruler is 50 cm long; pencil is 13 cm long.

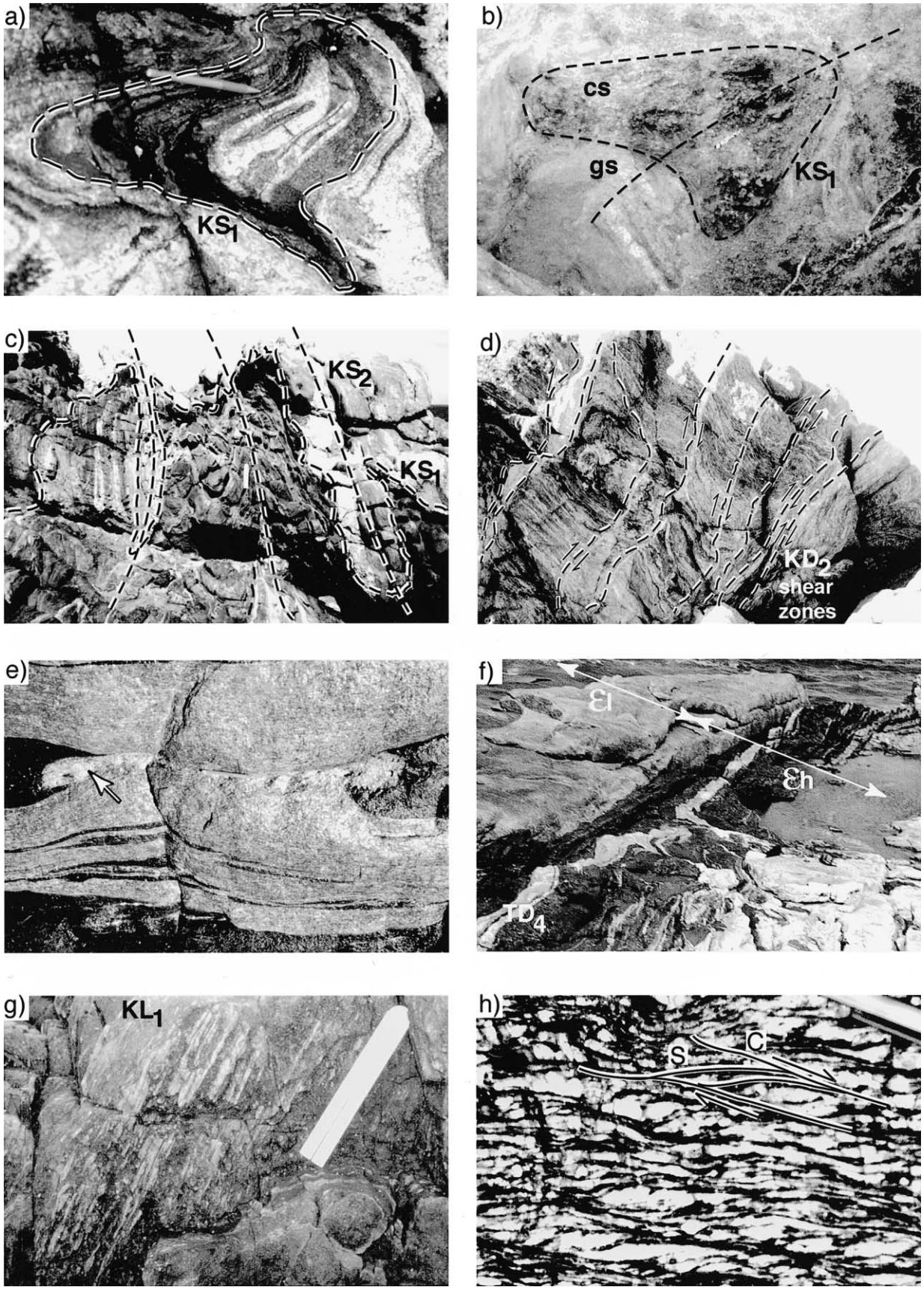
a)
KS1
b)
cs
gs
KS1
c)
KS2
KS1
d)
KD2
shear
zones
e)
f)
εl
εh
TD4
g)
KL1
h)
S
C

described below in Section 3.4 (Parker and Lemon, 1982; Parker et al., 1988). We observed these features in the Cleve–Cowell area (Poornamookinie Creek; Parker et al., 1988) and along the coast from Port Neill to Whalers Way (Figs. 3 and 4).

SHRIMP U–Pb zircon dating indicates that a high-grade thermal event occurred at ~2400 Ma, labelled the Sleafordian Orogeny (Thomson, 1980). The kinematics of the Sleafordian Orogeny are unclear. It was postulated that Sleafordian deformation was preserved in the Sleaford Complex as a high-grade compositional layering SlS_{0-1} developed by transposition of SlS_0 by SlS_1 during a phase of isoclinal folding (Parker et al., 1988). Isoclinal folds that fold this early fabric were attributed to SlD_2 (Drexel et al., 1993). However, Kimban high-strain zones have reactivated and transposed Sleafordian structural elements in the eastern Eyre Peninsula rendering the Sleafordian structures indistinguishable from the later ones. Structural development is identical in the Sleaford Complex, Lincoln Batholith, Hutchison Group and across the Kalinjala Shear Zone. Monazites collected from high-strain zones in

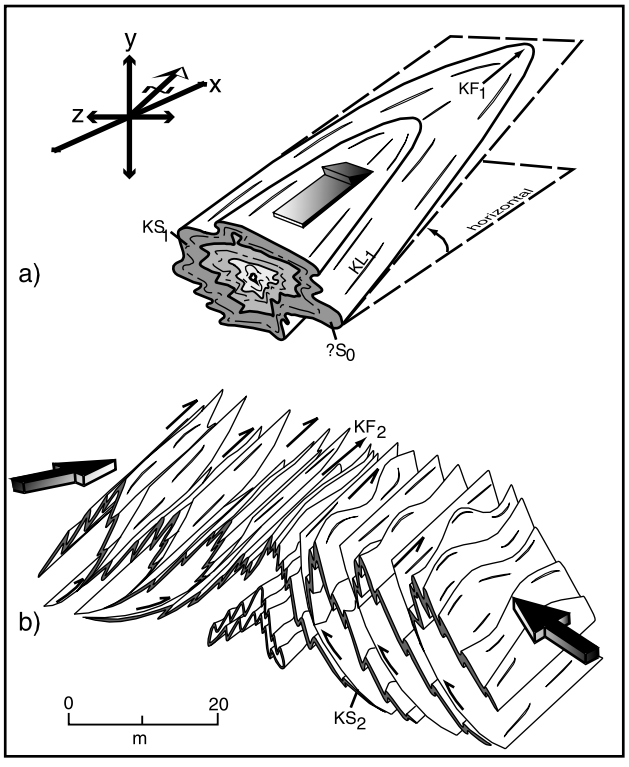

Fig. 7. Schematic development of structures related to the Kalinjala Shear Zone during the Kimban Orogeny. (a) Development of sheath folds during KD_1 representing the highest strain structures in the belt, with $X \geqq Y \geqq Z$ being the principal axes of strain. Bulk tectonic transport (X) appears to lie along a northeast–southwest plane with top-to-the-north shearing. (b) A representation of KD_2 structures developed as a function of increased flattening of the terrane. The sheath folds were overprinted by upright and overturned chevron folds developed due to overall thickening of the rock package by shear zones. Strain partitioning led to the development of both strike–slip and dip–slip shears.

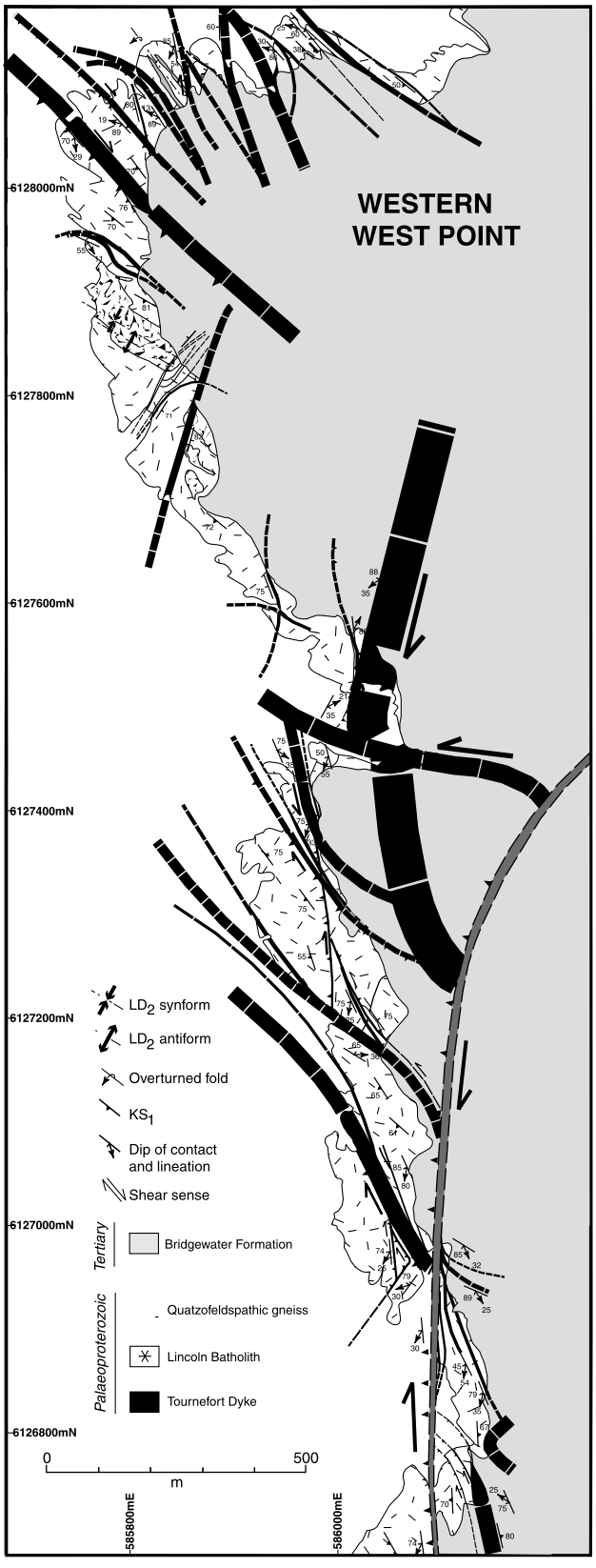

Fig. 8. Map of the western side of West Point (see Fig. 3), highlighting the prevalence of shear zones localised in the Tournefort dykes. This suggests that the mafic dykes were zones of mechanical weakness during the Kimban Orogeny concentrating the highest strains in them, as shown in Figs. 6(f) and 14.

Sleaford Complex layered garnet gneisses (dated using the SHRIMP U–Pb method) recorded an age of ~1710 Ma (Fanning and Aleinikoff, 1997). We interpret this age to reflect Kimban high-temperature shearing in the Archaean rocks. Moreover, identical structures also occur in the 1810 Ma Tournefort dykes. Therefore, the structures attributed by earlier workers to have formed during the Sleafordian Orogeny, in the areas described in this study, must have formed during the Kimban Orogeny [Fig. 6(a)–(h)].

3.1. First generation Kimban structures KD_1

The first generation of structures we recognise (KD_1) are a series of gently to steeply-plunging KF_1 mesoscopic non-cylindrical folds, or sheath folds (Figs. 6–8). KF_1 folds are pervasive throughout the terrain and in many cases are difficult to identify because they have been transposed, dismembered, or refolded. Regionally, KD_1 structures appear to have had an identical progressive development at amphibolite facies grades in the

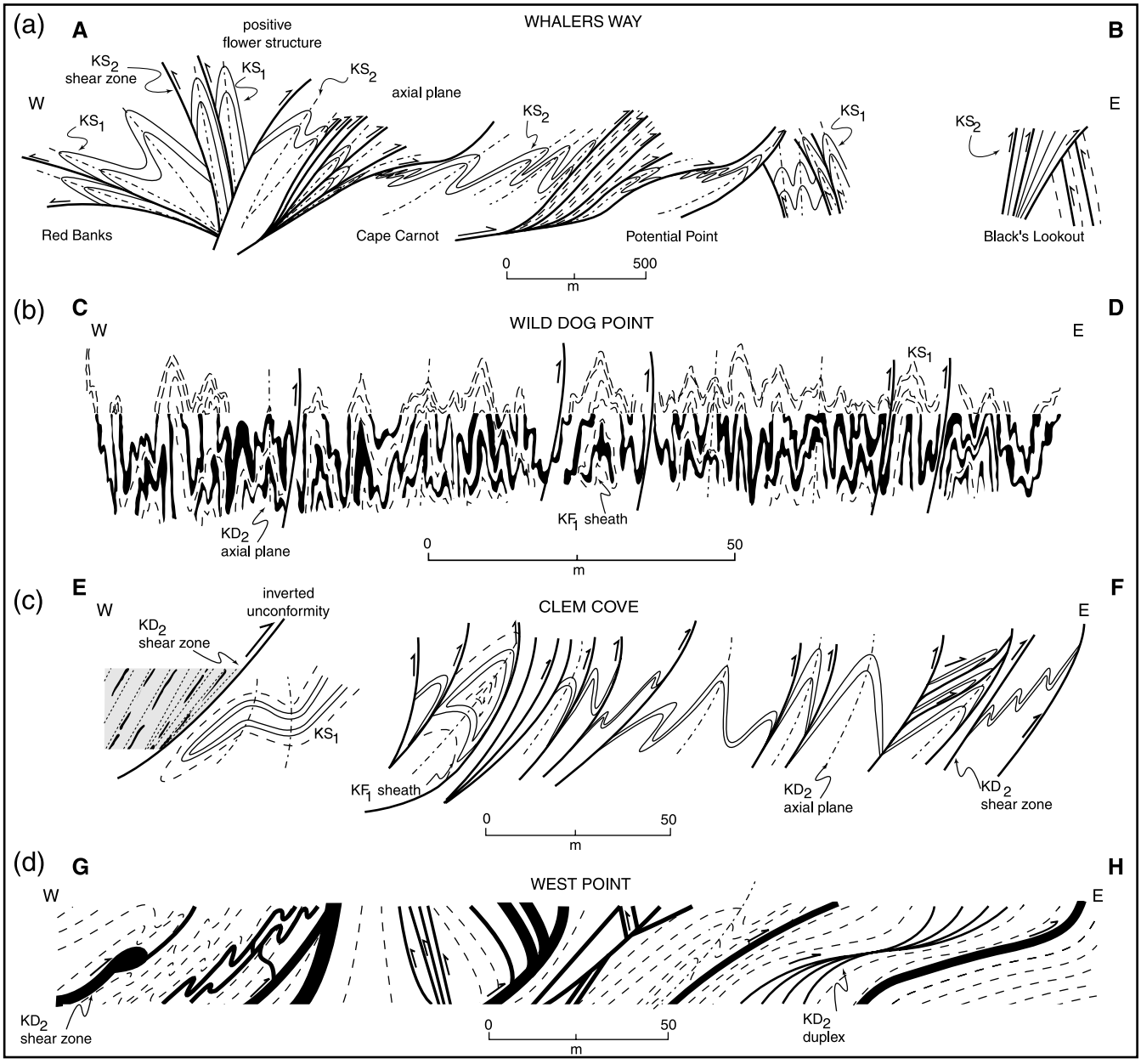

Fig. 9. Schematic cross-sections showing the structures developed during the Kimban Orogeny. Section locations are shown in Fig. 3. Large curved basal shear zones connect with smaller shears controlling meso-scale structural development. (a) A section through the Sleaford Complex at Whalers Way, with strain localised along KD_2 west-dipping reverse shears. (b) Structures in a domain dominated by KD_2 flattening structures as shown by the tight to isoclinally folded mafic dykes. Shortening is estimated at 85%; after Miller (1999). (c) Section showing the Archaean Sleaford Complex overlying the Palaeoproterozoic Hutchison Group at Clem Cove. (d) A representative section through the Lincoln Batholith showing the localisation of strain into the mafic dykes at West Point.

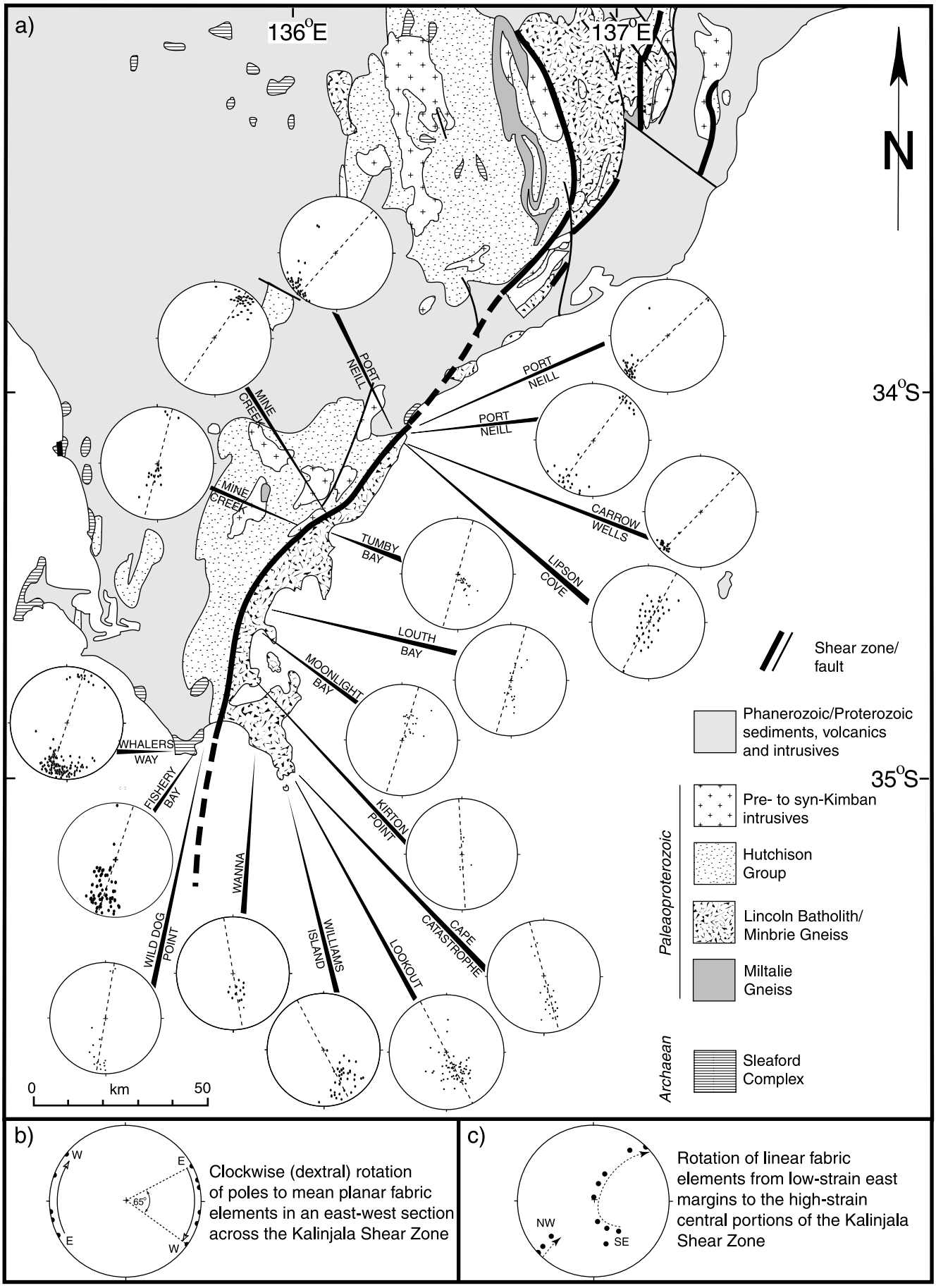
a)
136°E
137°E
N
34°S
35°S
PORT NEILL
MINE CREEK
TUMBY BAY
CARROW WELLS
LIPSON COVE
LOUTH BAY
MOONLIGHT BAY
WHALERS WAY
FISHERY BAY
KIRTON POINT
WANNA
WILD DOG POINT
WILLIAMS ISLAND
LOOKOUT
CAPE CATASTROPHE
0 km 50
Shear zone/ fault
Phanerozoic/Proterozoic sediments, volcanics and intrusives
Paleaoproterozoic
Pre- to syn-Kimban intrusives
Hutchison Group
Lincoln Batholith/ Minbrie Gneiss
Miltalie Gneiss
Archaean
Sleaford Complex
b)
W
E
65°
E
W
Clockwise (dextral) rotation of poles to mean planar fabric elements in an east-west section across the Kalinjala Shear Zone
c)
NW
SE
Rotation of linear fabric elements from low-strain east margins to the high-strain central portions of the Kalinjala Shear Zone

Cleve–Cowell area and the granulite grades in the southern portions of the belt.

Sheath folds range from those with sub-circular to tightly folded 'boomerang-shaped' sections perpendicular to their long axes [Fig. 6(a) and (b)]. Sheaths with sub-circular sectional shapes are rare and are only preserved in zones that did not suffer significant later flattening strains, such as at Fishery Bay (Fig. 3). Sheath sectional diameters range from 2 cm up to 5 m across and fold hinges culminate both to the north and south. The abundance of asymmetric, meso-scale sheath fold secondary and tertiary closures throughout the belt suggests that they are part of larger regional-scale structures. Kinematic indicators such as δ- and σ-winged in-plane porphyroclasts and porphyroblasts suggest that transport was driven by top-to-the-north shearing. The prevalence of gently south-plunging fold axes suggests that regional-scale south-plunging sheath folds occur along the margin of the Kalinjala Shear Zone. As the Kalinjala Shear Zone is a subvertical structure and the sheath fold *X*-axes are parallel to the gently plunging KL_1 the regional-scale structures may best be described as nappes.

Fold plunges/sheath fold long-axes parallel a primary linear fabric (KL_1) defined by prolate-shaped mineral aggregates [Fig. 6(g)]. Most linear clasts are composed of both quartz and feldspar with lesser proportions comprising pyroxene–amphibole-brown biotite or garnet/brown biotite aggregates. Lineations (also sheath fold long axes) parallel the strike of the sub-vertical Kalinjala Shear Zone, trending northwest in the south and rotate clockwise to the northeast in the north (Fig. 9). Linear surface traces trend north at Whalers Way and rotate clockwise along the Spencer Gulf to the northeast. Linear feldspar clasts have aspect ratios of up to 30:1 and a mean of 5:1 (Table 2) indicating that KD_1 was the highest strain event. One spectacular example of a sheath fold crops out at Lookout (Fig. 3) where a cone-shaped fold with a sub-horizontal long axis has an amplitude of 15 m. Many localities contain more highly deformed sheaths such as Cape Tournefort, Wanna, Sleaford Bay, Whalers Way, Tumby Bay and Lipson Cove (Fig. 3).

A strongly developed, high-grade, mylonitic foliation KS_1 mimics sheath fold cone geometries and lies sub-parallel to the lithological layering. This layering may possibly be S_0 or, more likely, an earlier high-strain surface that transposed the original layering during the Sleafordian Orogeny. Depending on the lithological association, KS_1 may be defined by a number of minerals such as pyroxene, amphibole, biotite, feldspar and quartz. The main orientation of KS_1 was probably sub-horizontal, though it now is primarily sub-vertical. On the meso-scale, high-grade ortho-pyroxene–sillimanite–amphibole–garnet–biotite–feldspar–quartz fabric planar fabrics are crenulated or completely transposed by KS_2. Pre- to syn KD_1 leucosomes lie parallel to KS_1 and contain garnet and amphibole porphyroblasts.

The prevalence of shear zones in pre-existing Tournefort dykes suggests that the dykes were zones of mechanical weakness during KD_1 [Fig. 6(f)]. Shear fabrics are weaker along dyke margins and are indistinguishable from earlier fabrics preserved in the encompassing metagranitoids less than 1 m from the zone. The widest sheared dykes always have greater offsets than the thinner ones. Where dykes have en échelon segmented geometries, shearing is translated to the next segment along discrete ultramylonites and the surrounding felsic material records no strain. Dykes that were initially very close ($<$1 m apart) were amalgamated to form $\sim$10 m wide shears consisting of up to ten dykes. The intervening metagranitoid tongues were drawn out into very thin felsic stringers ($>$2 cm wide) and quartz–feldspar rods up to 0.5 m long. On the microscopic scale undeformed domains 1 mm wide are commonly wrapped by intensely sheared fabrics. Where there are few dykes, strain is focussed along metagranitoid lithological boundaries.

3.2. Second generation Kimban structures (KD_2)

Second generation structures attributed by us to have formed during the Kimban Orogeny (KD_2) are characterised by curvilinear high-strain zones and tight to isoclinal upright and overturned chevron folds (Figs. 6–9). KD_2 structural domains verge both to the west and east, are listric and commonly form hinterland dipping or strike–slip duplexes. Shear zone strikes rotate from the northwest–southeast in the south to northeast–southwest in the north, parallel to the Kalinjala Shear Zone.

Two shear zone sets developed during KD_2, one with dextral and the other with sinistral offsets. The dextral shear zones dip steeply to the west and have quartz–feldspar–amphibole KL_2-fabrics that plunge $\sim$20–88° to the southwest. Oblique reverse movements are suggested by rotated winged in-plane σ- and δ-clast sense of shear indicators and $S \wedge C$-planes [Fig. 6(h)] along dyke/metagranitoid contacts. Link structures curving off the primary shear plane commonly have a ramp-flat geometry (e.g. Whalers Way; Fig. 9). Ramps dip to the south and lineations plunge 10–40° to the south, indicating south-over-north overthrusting. Ramp offsets are commonly about 10 m as recorded by offset marker dykes. These frontal ramp shear zones are stacked forming hinterland dipping duplexes in response to bulk strike–slip shearing. Therefore, oblique transport was partitioned into an interconnected array of both strike–slip and dip–slip shears [Fig. 6(d)]. Shear-plane solution data using the Finite Strain from Fault-slip

Fig. 10. Variation of lineation plunges throughout the Kimban Mobile Belt. (a) Lineations predominantly plunge south in the southern areas with an increase in northerly plunges to the north. (b) Regional average fabric trends rotate in a clockwise manner from low- to high-strain domains, indicating regional dextral shear. (c) Lineation plunges vary from gentle at Whalers Way to steep in the Lincoln Batholith suggesting the Kalinjala Shear Zone is triclinic.

Data method (FSDS; Cladouhos and Allmendinger, 1993) suggests that the principal pole of stress (*P*-pole) for deformation during this event was from the southwest 30°/220°. This interpretation is consistent with overall field observations of transport towards the northeast [Figs. 10(a), (b) and 11]. Offset marker dykes, rotated feldspar porphyroclasts and $S \wedge C$ fabrics also indicate a component of sinistral shear in northwest-trending high-strain zones with offsets up to 50 m. The sinistral shears are commonly transected, or were reactivated, by dextral shears. However, we consider them to have formed synchronously with the dextral shears because the overprinting relationships are not consistent across the belt. In zones of very high-strains, extensional shear bands (C'-planes) developed and the hinges of asymmetric folds are parallel to the elongation lineations. Coupled with steeply (70°) to gently (15°) plunging, south-dipping feldspar–quartz and amphibole elongation lineations (KL_2), the shear sense indicators suggest an oblique west-directed tectonic transport direction, with the east block overriding the west. The constructed FSDS pole lies at 26°/080°. The strike of both sinistral and dextral KD_2 shear zones are also sub-parallel to KL_1 surface traces suggesting that the two shear zone sets developed synchronously as an interconnected array during KD_2.

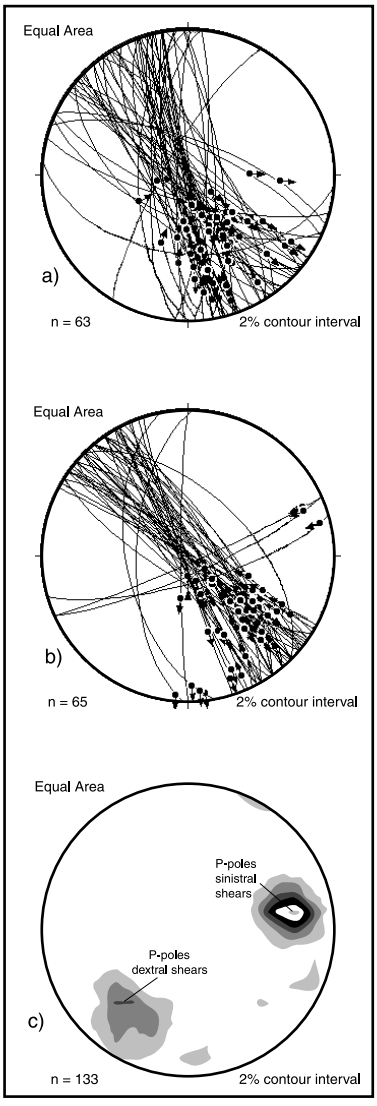

Fig. 11. Measured mesoscopic shear zones in the Lincoln Batholith with corresponding stretching lineations and vector arrows for: (a) dextral shear zones; and (b) sinistral shear zones. (c) Calculated poles of compression (*P*-poles) for the shear zones using the finite strain from fault-slip data method (Cladouhos and Allmendinger, 1993).

KD_2 folds are bounded by shear zones, are asymmetric, overturned and commonly recumbent. The underlying fold limbs are overturned and drawn into the shears. Fold wavelengths range from 10 cm to 50 m. Fold axes plunge gently to the north and south, commonly sub-parallel to KL_1. In the Lincoln Batholith KD_2 shear zones commonly reactivated KD_1 shear zones in the dykes. Where dykes are absent, lenticular medium-grained quartz–feldspar pegmatitic leucosomes acted as zones of preferential mechanical weakness and were sheared to form conjugate quartz–feldspar ± garnet ultramylonites (~2 cm wide and ~2 m long).

KS_2 surfaces in mafic dykes are defined by dark to pale-green amphibole (0.5 mm long) and pleochroic biotite that reactivated or completely transposed KS_1 by microshearing. In the highest strain zones C' microshears overprint the fabric and recrystallize the amphibole and plagioclase while opaque oxides form granular (25 mm in diameter) aggregates. KS_2 fabrics in the metagranitoids mainly consist of elongate quartz and feldspar aggregates. Deformed feldspars contain multiple mechanical deformational twins, with rare examples of grains bent along their length. In these instances, orthoclase has been transformed to microcline and plagioclase has undulose extinction.

3.3. Boudinage

Numerous boudinage structures occur throughout the belt ranging from brittle boudins to pinch and swell structures (Fig. 12). Many of the boudin networks may be described as chocolate tablet boudinage structures with sub-vertical long axes that deform KS_1, and transect KD_1 sheath folds, suggesting that they formed syn- to post-KD_1. These relationships will be discussed at the end of this section.

Brittle boudinage is most commonly observed in thin (<20 cm) dykes that are highly fragmented with some separations of 0.5 m almost equalling the length of the fractured dyke segment. Segment length to width aspect ratios are >5:1. Boudin necks are rectangular and medium-grained quartz–feldspar–biotite ± tourmaline leucosomes formed in the neck zone. The surrounding metagranitoid lithologies are not drawn into the neck zone and show little evidence of ductile deformation. These boudins have been overprinted by 'pinch and swell' structures suggesting that in a sequence of boudin types, these were the first to form.

Wider dykes (>20 cm) have larger separations and a 'fish-head' neck geometry. In many cases neck fracture

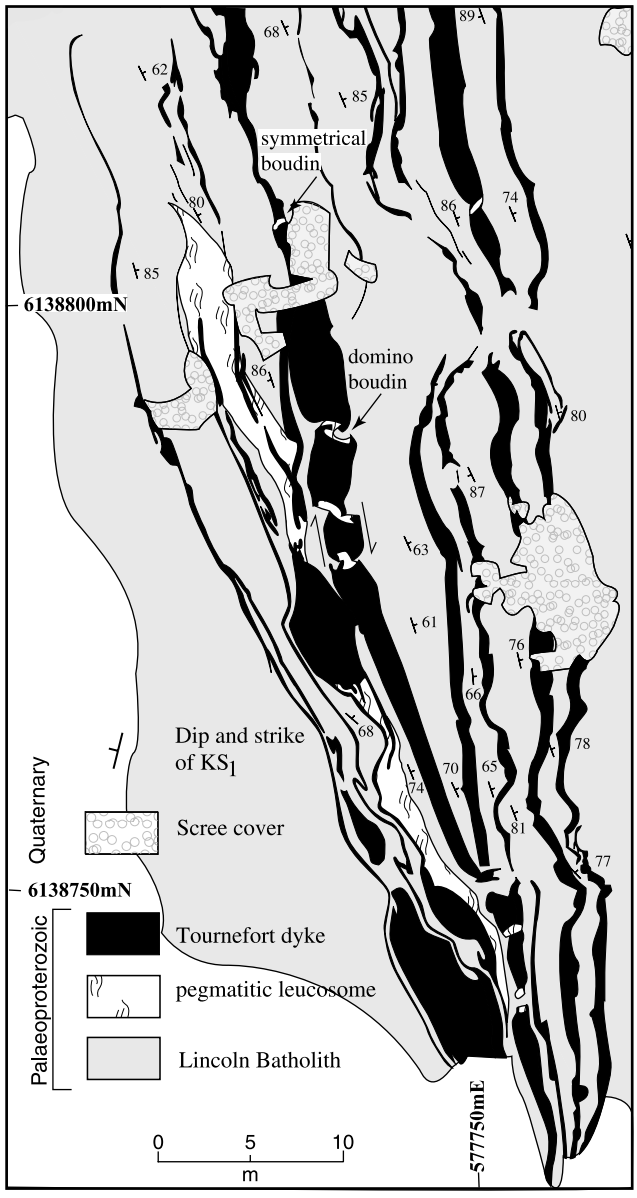

Fig. 12. Boudinage of mafic dykes in megacrystic orthogneiss at Wanna. Boudinage reactivation is shown by groups of fractured mafic dykes with 'fish-mouth' necks overprinted by 'pinch and swell' structures; after Bales (1996).

lines are sub-perpendicular to the dyke length indicating that almost pure tension initiated and continued boudin development (Ghosh, 1993; Sengupta, 1997). Fish-head boudins require a component of shear along the fracture segment margins for strain to be compatible across the lithological interface (Ghosh, 1993). The boudin necks of these structures contain coarse-grained pegmatite and quartz cores. There is a relationship between dyke width and boudin neck separation. Wider dykes (>3 m) have systematically larger separations and aspect ratios are >10:1. At Wanna one large dyke has a separation of >15 m and only the neck and one segment were observed. Zircons collected from leucosomes outcropping at Williams Island, have been dated using the SHRIMP U–Pb method (Vassallo, unpublished data) and suggest an age of ~1700 Ma when mineral blocking temperatures where reached.

Mafic dykes that are 'pinch and swelled' indicate that the dykes became increasingly more ductile during deformation as they overprint earlier brittle boudins. This increase in dyke ductility suggests there was an inversion in rheological behaviour of the dykes with respect to the metagranitoids (i.e. the metagranitoids began to behave more competently than the dykes). A relative rheological inversion of contrasting rock types during peak conditions is thought to suggest an increase in strain and temperature (Ghosh, 1993). Pinch zones are ~1 m wide and the swelled portions are >5 m wide. Pinch and swell aspect ratios are <5:1. In the most highly strained pinch zones the pinching gave way to brittle fracture of the metagranitoid and infilling of the neck with very coarse-grained quartz–feldspar–biotite pegmatitic leucosomes. Several spectacular examples occur at Wanna (Fig. 12) where the earlier-formed brittle dyke fracture necks have been ductily drawn into the pinched boudin necks, reactivating the earlier structure. Reactivated boudins are also found on Williams and Wedding Cake Island (Fig. 3).

The occurrence of numerous boudinaged dykes appears to be at odds with our earlier descriptions that many N–NW-trending dykes behaved as relatively weak anisotropic bodies that localised shear zone development. It is clear in many instances that the boudin necks do deform, or crosscut the KS_1 shear fabrics in the dykes, whereas at most only very weakly developed fabrics transect the leucosomes in the boudin necks. Therefore, we may only conclude that boudinage was synchronous with, or post-dated KD_1. A more specific solution to this problem may be found in Fig. 12, with the structure labelled 'domino boudin' located on a dyke that has also been symmetrically boudinaged. Goscombe and Passchier (2001) suggested that domino boudins can be used as indicators of flow regime, by: (1) highlighting the *X*-axis of the strain ellipsoid, which lies orthogonal to the long axis of the boudin neck line and in the enveloping surface; and (2) behaving as a kinematic indicator. Domino boudins have slip in the neck zone (at high-angles to the enveloping surface) that is antithetic to the bulk shear flow in a non-coaxial deformation where they lie in the *X*–*Y*-plane of the strain ellipsoid. Symmetrical boudins may also form in non-coaxial transpressional regimes where they are coincident with the *X*–*Y*-plane. Therefore, boudinage in the dykes may have been synchronous with KD_1 dextral shear that was preferentially localised in the metagranitoid after shearing occurred in dykes (that were in an orientation that was preferential for shear zones to develop). This partitioning of strain is due to the initial planar anisotropy of the dykes, followed by a rheological change that focussed shearing in the metagranitoids.

Another relationship highlights the synchronicity of shearing in the metagrantoids and dyke boudinage during KD_1. In areas of high-strain (e.g. Lookout): (i) KS_1 is

Table 1
Comparison of fabric nomenclature used in the Sleaford Complex, Lincoln Batholith, Hutchison Group and Kalinjala Shear Zone in southern Eyre Peninsula with those observed in central Eyre Peninsula (Parker and Lemon, 1982)

This study				Parker and Lemon (1982)			
				KD_3	KS_3	Open folds intensifying into sheath folds	
KD_2	KS_2	Reverse shearing and upright chevron folding boudinage	Verging to KSZ from the margins	KD_2	KS_2	Recumbent folds	West verging folds
KD_1	KS_1	Gently south-plunging sheath folds	North verging	KD_1	KS_1	Layer-parallel fabric	?

strongly developed; (ii) mafic dykes are highly fragmented (boudin offsets can be >50 m) and the fabric tightly envelopes them; and (iii) shear zone offsets are large (>100 m). Low-strain zones (e.g. West Point), show weak foliation development, small boudin separation (<3 m) and small shear zone offsets.

3.4. Comparison of structural models for the Kimban Orogeny

The Kimban Orogeny was originally defined by to a series of high-strain structures in Hutchison Group metasediments that crop out in the central Eyre Peninsula (Parker and Lemon, 1982). However, our observations (presented above) significantly differ from that (currently accepted) structural scheme. Parker and Lemon's (1982) model consisted of three deformation events KD_1, KD_2 and KD_3 that occurred during one prolonged metamorphic event (Table 1). KD_1 was inferred by the presence of KS_1, a penetrative, layer-parallel, muscovite–biotite–sillimanite fabric that forms inclusion trails in syn- or post-KD_1, pre-KD_2 garnet and andalusite porphyroblasts. Parker and Lemon (1982) did not believe that any folds formed during this event. Our interpretation disputes this idea and highlights that the first event KD_1 that formed KS_1 was the highest strain event in the region and its accompanying high-grade sheath folds are of regional tectonic significance and formed during the evolution of the Kalinjala Shear Zone.

KD_2, interpreted by Parker and Lemon (1982) as an amphibolite to granulite facies event, was thought to have produced asymmetric recumbent isoclinal folds that verge to the west. Corrected for refolding, fold axes plunged gently to 010–020° and are parallel to the KL_2 mineral elongation lineation. An axial surface schistose fabric, KS_2, crenulates or transposes KS_1. Transposition along KD_2 fold limbs led Parker and Lemon (1982) to infer the presence of east-dipping reverse shear zones. Our observations indicate that KD_2 reverse shear zones verge to the west and east as a function of flattening during the transpression.

The third deformation, KD_3, was envisaged to have been a heterogenous strain event. Open regional upright folds were believed to have tightened to form sheath folds approaching the Kalinjala Shear Zone (Parker, 1980; Parker and Lemon, 1982). We find no evidence to suggest a third deformation event occurred during the Kimban Orogeny, but rather that these structures belong to KD_2 as folds they had ascribed to KD_2 are dissected sections of KD_1 sheath folds. The apparent KD_3 sheath folds associated with the Kalinjala Shear Zone are retrogressed KD_1 sheaths.

4. Strain calculations

Determination of three-dimensional finite strain in highly deformed plutonic igneous rocks that have attained granulite facies metamorphic conditions is challenging as the traditional methods of analysis used in sedimentary rocks (e.g. using deformed fossils, balancing cross-sections) cannot be applied. Qualitative methods such as fabric evolution studies have been applied in the past, yet these only provide broad estimates and relative measures of the state of strain in a rock if specific parameters cannot be measured (Jezek et al., 1996; Schulmann et al., 1996). Even though strain estimation in granulites is fraught with assumptions (primarily related to changes in volume due to melt loss during dehydration or fluid gain during retrogression), we attempted four semi-quantitative methods to define Kimban deformation (where $X \geqq Y \geqq Z$). These methods are: (i) Fry analyses; (ii) analysis of deformed microgranitoid enclave length-to-width ratios; (iii) measurement of deformed porphyroblasts and porphyroclast dimensions; and (iv) shear strain calculations in discrete shear zones.

4.1. Fry analyses

Fry analysis (Fry, 1979) is based on the centre–centre separations of clasts in a deformed matrix and how these approximate a finite strain ellipse in two dimensions. Three dimensional strain analyses are achieved by combining the measured results of at least two orthogonal planes (i.e. *XZ*-plane and *XY*-plane). Fry's method is most commonly

Table 2
Fry analyses completed on rocks from Williams Island and Wanna. Syntectonic strains were in areas that we identified as not having been deformed during the Kimban Orogeny. ϵl = low-strain, ϵm = moderate-strain, ϵmh = moderate- to high-strain and ϵh = high-strain as determined by fabric intensity. See Fig. 13 for their location on a logarithmic Flinn plot. All these samples have been moderately affected by KD_2

	Syntectonic	ϵl	ϵl	ϵm	ϵmh	ϵmh
log *Y/Z*	0.30	0.18	0.54	0.43	0.52	0.63
log *X/Y*	0.30	0.17	0.43	0.48	0.53	0.60

applied to low-grade rocks and may be applicable for use megacrystic metagranitoids if the feldspar porphyroclasts were initially uniformly distributed prior to deformation (Ramsay and Huber, 1983), and total accumulated strains are no greater than ~7:1. The first assumption is that there are no pre-Kimban fabrics in the rock. Even though this is clearly not the case, because of the pre-existing weak syn-Lincoln fabrics, the pre-Kimban strains in the Lincoln Batholith are minimal and have not significantly affect the results (Table 2). The second assumption is of greater significance as in the higher strain zones where strain ratios are >7:1, C'-planes cut the clasts, effectively increasing the number of centres and therefore invalidating the method. The inability to analyse the highest strains in the rock leads to a large under-estimate of the bulk state of strain. Despite these inherent limitations the method is still useful for determining the shape of the strain ellipsoid and a determination of the bulk ratio of strain in the metagranitoids recorded in low-strain zones.

Table 2 shows the results of six different Fry analyses completed in areas of relatively low bulk finite strain. Increasing strain (ϵl to ϵmh; Table 2) is marked by an increased fabric intensity and greater microscopic grain refinement. $S \wedge C$-planes began to develop in zones classed to have suffered medium strain intensities (ϵmh). The results presented in Table 2 are plotted in Fig. 13. The Fry analyses plot very close to the $K = 1$ line suggesting that in low-strain sites, bulk strain was plane strain even with up to 30% loss of original rock volume.

4.2. Deformed enclave measurements

Analysis of microgranitoid enclave length-to-width ratios were completed in order to gain some overall magnitude of strain ellipticity ratios in individual shear zones. The advantage of this method is that grain refinement does not significantly affect the analytical results as the enclaves were already fine-grained prior to the deformation. The principal assumption in using this method is that most enclaves had approximately the same ellipticity before deformation. Many studies gauging enclave ellipticities in undeformed granitoids determine variable emplacement strains throughout plutons (e.g. Vernon et al., 1983). Thus, it is clear that measurement of tectonically strained enclaves must be accompanied by measurement of nearby undeformed samples.

One rare example of this relationship occurs on the south-western side of Williams Island. There, a north-trending KD_2 shear zone in Lincoln Batholith metagranitoids has a weakly deformed area along its western margin. In this area one dozen undeformed enclaves have an average length-to-width ratio of ~2:1. In the centre of the shear zone ~50 enclaves are highly attenuated (Table 3). Dimensional measurements in the *XZ*-plane produced an average *X/Z* ratio of 20.5 in the areas of highest strains. Comparing fabric development, this shear is of moderate strain compared to those localised in the mafic dykes and suggests that *X/Z* ratios of >20 are common in the dykes.

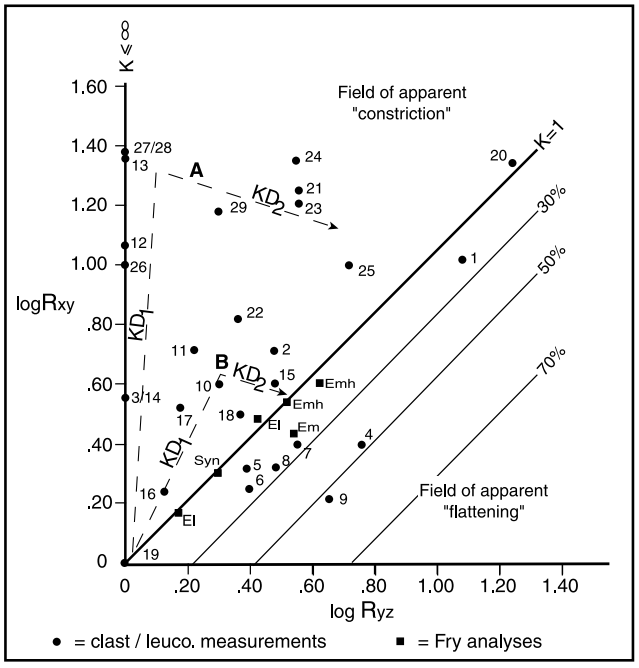

Fig. 13. A logarithmic Flinn plot showing the progression of clast shape with increasing strain during the Kimban Orogeny. Original starting shapes of clasts are either undeformed, or were modified by plane strain during the Lincoln Orogeny in the Lincoln Batholith (c.f. Table 2). In the pre-1850 Ma rocks (data points 1–9) the effects of the Sleafordian Orogeny are considered minimal as only low-strain structures are preserved outside of the Kimban mobile belt. The effect of the postulated Miltalie Event on pre-1850 Ma rocks is unknown, though we believe it has had little impact on the results of this study as no major structures of that age have been identified in the belt. There is a transition from undeformed rectangular, or sub-spherical clasts/leucosomes in Kimban low-strain zones to those with highly prolate shapes, and less commonly plane strain shapes, in areas primarily deformed by KD_1 sheath folds, but only weakly affected by KD_2 structures. In areas strongly dissected by KD_2 shear zones, clasts fall primarily near the plane strain $K = 1$ line indicating that KD_1 was a much higher strain event than KD_2. However, the location of clasts affected by intense KD_2 structures, such as at Wild Dog Point, near the apparent field of 'flattening', suggests that KD_2 had a high component of flattening compared to constriction during that event. This conclusion may be compared with Fig. 9 (section C–D) where dykes have been deformed by tight upright folds, also indicative of a high degree of flattening. The clasts are not oblate in shape as the intensity of deformation during the flattening event was not as great as the constrictional event. Those samples that plot to the right of the $K = 1$ line have all been moderately to strongly deformed by KD_2 structures. The outlines of the strain path in these granulites may be identified by relating the clast shape to specific structural generations (dashed lines). Path (A) is indicative of rocks that have accommodated highly-constrictional strains during KD_1 followed by flattening. Path (B) shows a path for rocks that have seen a greater component of plane strain during KD_1 compared to path (A), prior to KD_2 flattening. Loss of rock volume during deformation increases the field of apparent 'constriction' shifting the $K = 1$ line into the apparent field of 'flattening' as shown for 30, 50 and 70% volume loss.

4.3. Shear strain calculations (γ)

Two high-strain shear zones with highly evolved

Table 3
The dimensions of weakly deformed and highly deformed microgranitoid enclaves on the margins and in the centre of a mesoscopic shear zone. Strain ellipticity ratios (in the *X*–*Z*plane) suggest an average elongation of >7 times in the shear zone compared with its weakly deformed margins

Weakly deformed samples (13)			Enclave ellipticities			Highly strained samples (121)					
Axes short (cm)	Long (cm)	*XZ* ratio	Axes short (cm)	Long (cm)	*XZ* ratio	Axes short (cm)	Long (cm)	*XZ* ratio	Axes short (cm)	Long (cm)	*XZ* ratio
3	18	6.0	5.5	150	27.3	2.5	17	6.8	2.0	139	69.5
7	10	1.4	8.0	82	10.3	3.5	25	7.1	7.0	175	25.0
7.5	11	1.5	3.5	53	15.1	1.5	50	33.3	4.2	67	16.0
16	38	2.4	7.0	125	17.9	4.0	70	17.5	2.0	52	26.0
5	14.5	2.9	7.0	90	12.9	3.5	74	21.1	3.5	56	16.0
2	5.5	2.8	9.5	90	9.5	5.0	60	12.0	6.0	48	8.0
4	8	2.0	2.5	28	11.2	2.5	48	19.2	3.5	58	16.6
2.5	8	3.2	5.0	90	18.0	4.0	73	18.3	2.0	22	11.0
5.5	15	2.7	7.0	195	27.9	4.0	50	12.5	5.0	100	20.0
4	7.5	1.9	2.5	150	60.0	3.0	51	17.0	2.0	38.0	19.0
5	9	1.8	2.0	150	75.0	4.0	175	43.8	1.4	19.0	13.6
6	12	2.0	10.0	125	12.5	2.0	33	16.5	11.5	274.0	23.8
3	11	3.7	3.5	60	17.1	3.0	100	33.3	6.0	50.0	8.3
			10.0	100	10.0	1.5	36	24.0	2.0	24.0	12.0
Average *X/Z* ratio	2.6	10.0	315	31.5	5.0	76	15.2	5.5	50.0	9.1	
			8.0	270	33.8	1.5	76	50.7	2.5	40.0	16.0
			6.0	65	10.8	4.0	148	37.0	3.5	74.0	21.1
			10.0	250	25.0	3.5	85	24.3	2.5	62.0	24.8
			9.0	80	8.9	2.4	22	9.2	5.0	121.0	24.2
			6.0	115	19.2	5.0	82	16.4	5.0	105.0	21.0
			4.0	190	47.5	1.4	21	15.0	2.5	41.0	16.4
			7.0	150	21.4	1.0	18	18.0	3.2	25.0	7.8
			5.0	65	13.0	13.5	110	8.1	3.0	17.0	5.7
			9.0	158	17.6	2.3	81	35.2	6.0	71.0	11.8
			2.5	100	40.0	2.0	48	24.0	5.0	52.0	10.4
			6.0	255	42.5	4.5	46	10.2	3.0	22.0	7.3
			5.0	88	17.6	2.0	39	19.5	1.5	31.0	20.7
			13.0	260	20.0	3.5	56	16.0	4.0	38.0	9.5
			2.5	21	8.4	3.0	42	14.0	3.0	21.0	7.0
			2.5	135	54.0	1.0	23	23.0	5.5	71.0	12.9
			5.0	97	19.4	2.5	150	60.0	6.0	60.0	10.0
			6.0	100	16.7	1.0	14	14.0	4.0	71.0	17.8
			3.0	78	26.0	1.0	26	26.0	6.0	260.0	43.3
			4.0	75	18.8	1.3	40	30.8	3.5	82.0	23.4
			34.0	175	5.1	2.5	45	18.0	7.0	74.0	10.6
			8.0	122	15.3	5.5	142	25.8	3.4	50.0	14.7
			4.5	73	16.2	2.0	40	20.0	4.5	94.0	20.9
			7.5	56	7.5	1.4	39	27.9	7.0	67.0	9.6
			12.0	58	4.8	1.6	60	37.5	4.5	39.0	8.7
			7.0	70	10.0	2.8	48	17.1	4.7	75.0	16.0
			1.0	21	21.0						
									Average *X/Z* ratio	20.5	

C'-plane fabrics crosscut by two thinner dykes perpendicular to them were analysed to determine the amount and nature of the strain (Fig. 14). Emplacement fractures of the thinner dykes are preserved between the two shear zones indicating little to no strain has been accommodated there. However, several metres either side of the low-strain zone, the thinner dykes curve sharply into the shears. Fig. 14 shows the strain intensity gradient in the two zones. Shear strain ($\gamma = \tan\psi$) increases towards the centre of the dyke as shown in the γ vs distance (m) from shear zone margin graph. This suggests that the shear zones nucleated in the centre of the dykes causing an inherent zone of weakness to develop on the nucleation plane. Therefore, strain was localised in the mafic units. One likely reason for the shear zones to nucleate in the dykes rather than the surrounding metagranitoids is that the interconnected array of crosscutting dykes throughout the belt acted as planes of anisotropic weakness during the beginning of deformation. This may have been enhanced by the original fine-grained nature of the dykes making them mechanically weaker than the coarser-grained porphyritic metagranitoids.

A marked strain gradient occurs along dyke margins and is compatible across the lithological contact. Strain ellipticity ratios were calculated by means of Mohr circle construction (Fig. 14), using singular observations of angular shear strain (ψ). Dilatation (Δ_A) is unknown using this method, thus only the ratio of the maximum (λ_1) and minimum (λ_2) finite stretches can be calculated. A dramatic

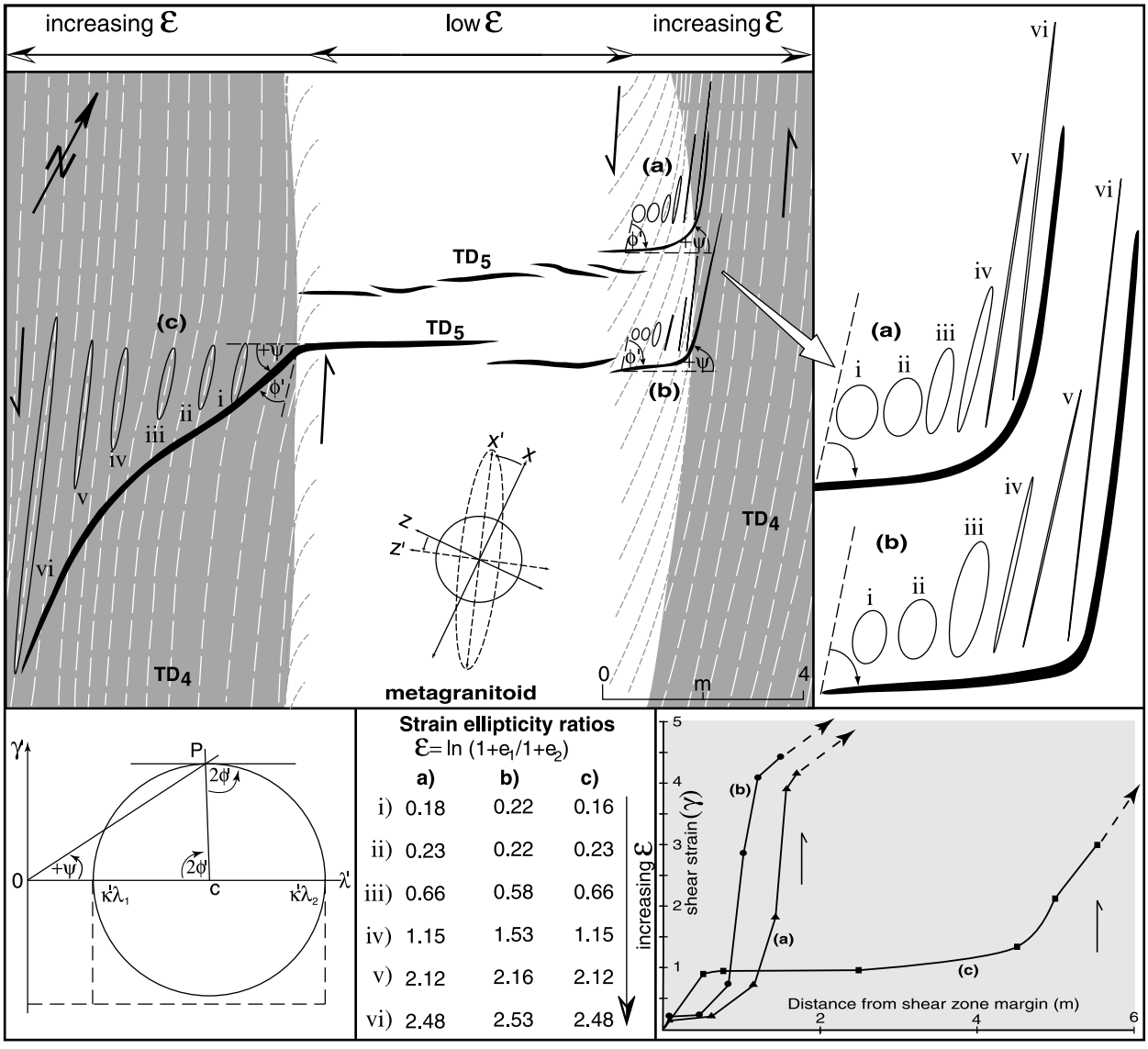

Fig. 14. Diagram showing the localisation of shear zones in Tournefort dykes. The field sketch shows two originally perpendicular sets of dykes. The wider dykes strike to the northwest, a favourable direction for shear zone generation. Where the two thinner dykes crosscut the wider ones, they are rotated in an anticlockwise direction indicating sinistral shear. Only low-strains were accommodated in the metagranitoid as shown by the preservation of the original dyke en échelon intrusion fracture sets. Strain ratio ellipses calculated using Mohr circles with a single value of angular shear strain are placed along the sheared dyke portions showing strain heterogeneity and strain localisation in the wider dykes. X–X' shows the rotation of infinitesimal stretching direction.

increase in stretching occurs in the dykes and the primary stretching axis rotates anticlockwise. These observations are important because these two zones are typical of the shear zones that are abundant throughout the belt. The largest observed offset in a mesoscopic shear zone is ~300 m on the western margin of Williams Island.

4.4. Deformed porphyroclast/porphyroblast/sub-spherical leucosome measurements

The abundance of megacrystic metagranitoids, and the occurrence of rare sub-spherical pre- to syn-KD_1 leucosomes in mafic dykes, in the belt allows us to determine strain over a wide area. This is most useful in attempting to classify the strain ratios in and along the margins of the Kalinjala Shear Zone (Table 4). Several deformed clast types and leucosomes were measured in X, Y and Z orientations. X is taken to represent the maximum finite stretching direction. Variations in clast/leucosome shape are plotted on a logarithmic Flinn plot (Fig. 13). Fig. 13 shows the plots of calculated mean $\log R_{XY}/\log R_{YZ}$ values along a section perpendicular to the strike of the Kalinjala Shear Zone. Based on field examinations, all measured samples have been strongly affected by KD_1 due to the presence of KS_1 throughout the area. However, the occurrence of KD_2 structures is more heterogeneously distributed and some sub-areas are more strongly affected by it than others. Therefore, Table 4 indicates the relative degree of KD_2 development in each sample area, in an attempt to correlate the field observations with the final plotted strain ratios. When examined in this light, a strong correlation emerges between the occurrence of KD_1 sheath folds in areas of low to moderate KD_2 strain (as determined by the intensity of KS_2 fabric development) and clasts from these areas that lie in the field of apparent 'constriction'. In areas strongly affected by KD_2 structures (e.g. Wild Dog Point), clast ratios plot along the line of plane strain ($K = 1$) or in the field of apparent 'flattening'. These correlations suggest that strain was not simply heterogeneous throughout the belt and random, but rather that two different definitive processes occurred in the development in the Kimban mobile belt.

The strain ratios suggest that strain was constrictional, to plane strain, during KD_1, which also clearly formed the KD_1 sheath folds. Several clasts lie in the plane strain and the field of apparent 'flattening' suggesting that a significant period of flattening followed the high constrictional strains during KD_2, indicating that the Kimban mobile belt is clearly a transpressional shear belt.

Table 4
Clast dimensions, ordered from west to east centred on the Kalinjala Shear Zone, showing the strain ellipticity ratios plotted in Fig. 13. See Fig. 10(a) for the location of study sites

No.	Clast type	Location	Sample size	Affect of KD2?	Dimensions (cm)					
					Z	*Y*	*X*	*X/Y*	*Y/Z*	*X/Z*
1	Feldspar	Trigg Point	15	Mod	0.2	2.4	25.0	10.4	12.0	125.0
2	Feldspar	Black's Lookout	30	Mod	1.0	3.0	15.5	5.2	3.0	15.5
3	Garnet	Fishery Bay	12	Weak	1.4	1.4	5.0	3.6	1.0	3.6
4	K-feldspar	West Sleaford Bay	20	Strong	0.7	4.0	10.0	2.5	5.7	14.3
5	Leucosome	Wild Dog Point	4	Strong	6	13	25	1.9	2.2	4.2
6	Leucosome	Wild Dog Point	10	Strong	5	12	20	1.7	2.4	4.0
7	Leucosome	Wild Dog Point	23	Strong	2	7	18	2.6	3.5	9.0
8	Leucosome	Wild Dog Point	49	Strong	2	6	13	2.2	3.0	6.5
9	Leucosome	Wild Dog Point	52	Strong	1	5	9	1.8	5.0	9.0
10	K-feldspar	Port Neill	30	Weak	1.5	3.0	12.0	4.0	2.0	8.0
11	K-feldspar	Carrow Wells	30	Weak	1.5	2.5	13.0	5.2	1.7	8.7
12	K-feldspar	Tumby Bay	25	Weak	0.6	0.6	7.0	11.7	1.0	11.7
13	K-feldspar	Tumby Bay	26	Weak	0.7	0.7	16.0	22.9	1.0	22.9
14	K-feldspar	Louth Bay	30	Weak	2.5	2.5	9.0	3.6	1.0	3.6
15	K-feldspar	Moonlight Bay	25	Mod	1.0	3.0	12.0	4.0	3.0	12.0
16	K-feldspar (Undef.)	Wanna	10	No	1.5	2.0	3.5	1.8	1.3	2.3
17	K-feldspar	Wanna	20	Weak	2.0	3.0	10.0	3.3	1.5	5.0
18	K-feldspar	Cape Tournefort	30	Mod	1.5	3.5	11.0	3.1	2.3	7.3
19	K-feldspar (Undef.)	Lookout	25	No	1.5	1.5	1.5	1.0	1.0	1.0
20	Feldspar	Lookout	200	Mod	3.0	3.5	60.6	22.1	17.3	20.3
21	Feldspar	Lookout	100	Weak	3.0	13.9	48.8	17.8	3.6	16.2
22	Feldspar	Lookout	100	Mod	3.8	25.3	15.2	6.6	2.3	4.0
23	Feldspar	Lookout	100	Mod	2.1	8.1	21.6	16.1	3.6	10.2
24	Feldspar	Lookout	100	Mod	2.3	12.9	42.7	22.4	3.5	18.5
25	Feldspar	Lookout	100	Mod	5.5	11.8	45.1	9.9	5.2	8.2
26	Amphibole	Cape Catastrophe	15	Weak	0.2	0.2	2.0	10.0	1.0	10.0
27	Feldspar	Cape Catastrophe	20	Weak	0.1	0.1	3.0	30.0	1.0	30.0
28	Amphibole	Cape Catastrophe	15	Weak	0.1	0.1	2.4	24.0	1.0	24.0
29	Feldspar	Cape Catastrophe	20	Weak	0.1	0.2	3.0	15.0	2.0	30.0

5. Development of a major crustal shear zone

The type-section for the Kalinjala Shear Zone is at Port Neill in central–eastern Eyre Peninsula (Parker, 1980). Examination of shear zones in the rock units along the southern margins of the belt show that they are prolific throughout all sequences. Parallel north-striking, reactivated, overthrust shears are the key elements of Kimban deformation. There are major shear zones transecting the Lincoln Batholith, Hutchison Group and Sleaford Complex along the southern coast. Strain distribution in them is highly heterogenous. Intensely developed S–L fabrics are commonly associated with the nearby occurrence of mafic dykes.

Aeromagnetic surveys of eastern Eyre Peninsula highlight a curvilinear aeromagnetic high broadly coincident with the Kalinjala Shear Zone type-section—it passes along the margin of the Spencer Gulf and through the centre of Sleaford Bay (Fig. 15; Drexel et al., 1993). Shear zones in the Sleaford Complex and Hutchison Group have a greater magnetic intensity than the surrounding rocks. One example lies on the western side of Sleaford Bay and has excellent exposure at Wild Dog Point (Fig. 3). Qualitatively, strain in this area is high as it contains an intense KS_1 gneissosity and many strongly boudinaged and tightly folded Tournefort dykes. The proportion of dykes at this headland is much greater than elsewhere along the Whalers Way coast. Magnetic imaging is ideal for locating large shear zones throughout the belt due to the relationship of the magnetically susceptible units and the occurrence of the highest strains. Parallel, north-striking, linear magnetic anomalies between Whalers Way and Coffin Bay are most likely to be major shear zones identical to the one preserved at Wild Dog Point.

Magnetic signatures of shear zones in the Lincoln Batholith are not as easy to identify due to the high background response of the metagranitoids. However, the contact of the magnetically quiet Hutchison Group and the Lincoln Batholith can be identified by the abrupt reduction of the magnetic signature sub-parallel with the western Spencer Gulf coastline. As the Kalinjala Shear Zone coincides with this contact, it is likely to represent a sheared lithological contact activated during KD_1 and reactivated during KD_2.

On the whole, the linear magnetic features on the aeromagnetic image represent the Kimban structural grain [compare Figs. 10(a) and 15]. An intensification of these elements coincides with a greater intensity of KD_1 structural elements and a narrowing of the belt to the south. Greater spacing between the linear elements in the northeastern Eyre Peninsula can be related to the more open KD_2 structures described by Parker and Lemon (1982) in the Cleve/Cowell area. Fig. 15 also shows the typical fold interference pattern found in outcrop scale on a larger scale, north of Whalers Way. The pattern suggests a sheath fold ~20 km in diameter refolded along a north-trending KD_2 axis.

Fig. 16 depicts the architecture of the region after the imposition of KD_2 strain. Thus, the Hutchison Group appears to lie in a westerly dipping tectonic wedge encompassed by two terrains, predominantly composed of orthogneissic material. The Kalinjala Shear Zone happens to coincide with an original nonconformity and is likely to have formed as a result of reactivation of a lithological boundary. That is, the Kalinjala Shear Zone was an unconformable contact activated during the Kimban Orogeny.

Terrains that are as complexly deformed as the Kimban Mobile Belt have three-dimensional variations in strain. Our investigations have focussed on the changes in the shape of the finite strain ellipsoid as structures evolved in the belt. We have concluded that strain initially consisted of sub-horizontal 'constriction' followed by a period of sub-horizontal 'flattening'. If the central high-strain portion of the Kalinjala is interpreted as having monoclinic symmetry, using the classification of Fossen and Tikoff (1998) accounting for constant-volume transpression (though we cannot gauge the true proportion of material gained or lost in these granulites), KD_1 and KD_2 fall into the type E (vertical shortening equals shear zone normal shortening causing a stretch along the X-axis) and type C (shear-plane flattening) transpression reference deformations, respectively. On the basis of this interpretation we have attempted to depict the material flow lines of the deformation (Fig. 17). This suggests that either sub-horizontal shortening dramatically increased (the coaxial deformation component), or sub-vertical shortening decreased as deformation progressed. If the Kalinjala Shear Zone is considered in the scheme of Passchier (1998) it may be described as a laterally constricted shear zone. According to that scheme the Kalinjala lies somewhere in between Y_I- and Z_I-type end members.

In natural shear zones structural complexities are to be expected due to inhomogeneous flow (Passchier, 1997; Jiang and Williams, 1998). Lin et al. (1997) suggest that segments of shear zones may approximate monoclinic flow, but when considered as a whole indicate triclinic flow. This can be determined in a shear zone by plotting its fabric elements (S, C, L) in high and low-strain domains. If L plots off the great circle defined by these elements, it indicates that the shear direction is oblique to the stretching direction and thus the shear zone is triclinic. In the field, the most notable feature of triclinic shear zones is the variation of stretching lineation plunge. Fig. 10(c) shows the variation in plunge of the stretching lineation across high- and low-strain domains of the study area, which suggests the Kalinjala Shear Zone is triclinic. We are not able to conclusively determine whether the Kalinjala is triclinic, due to the possible geometric interference of earlier structures. However, the rotation of KL_1 25 km across strike from gentle (10°S) in the central high-strain region (Sleaford Complex) to steep (90°SE) in the low strain margins (Lincoln Batholith) suggests that strike–slip and dip–slip partitioning did occur. The partitioning of the shear zone

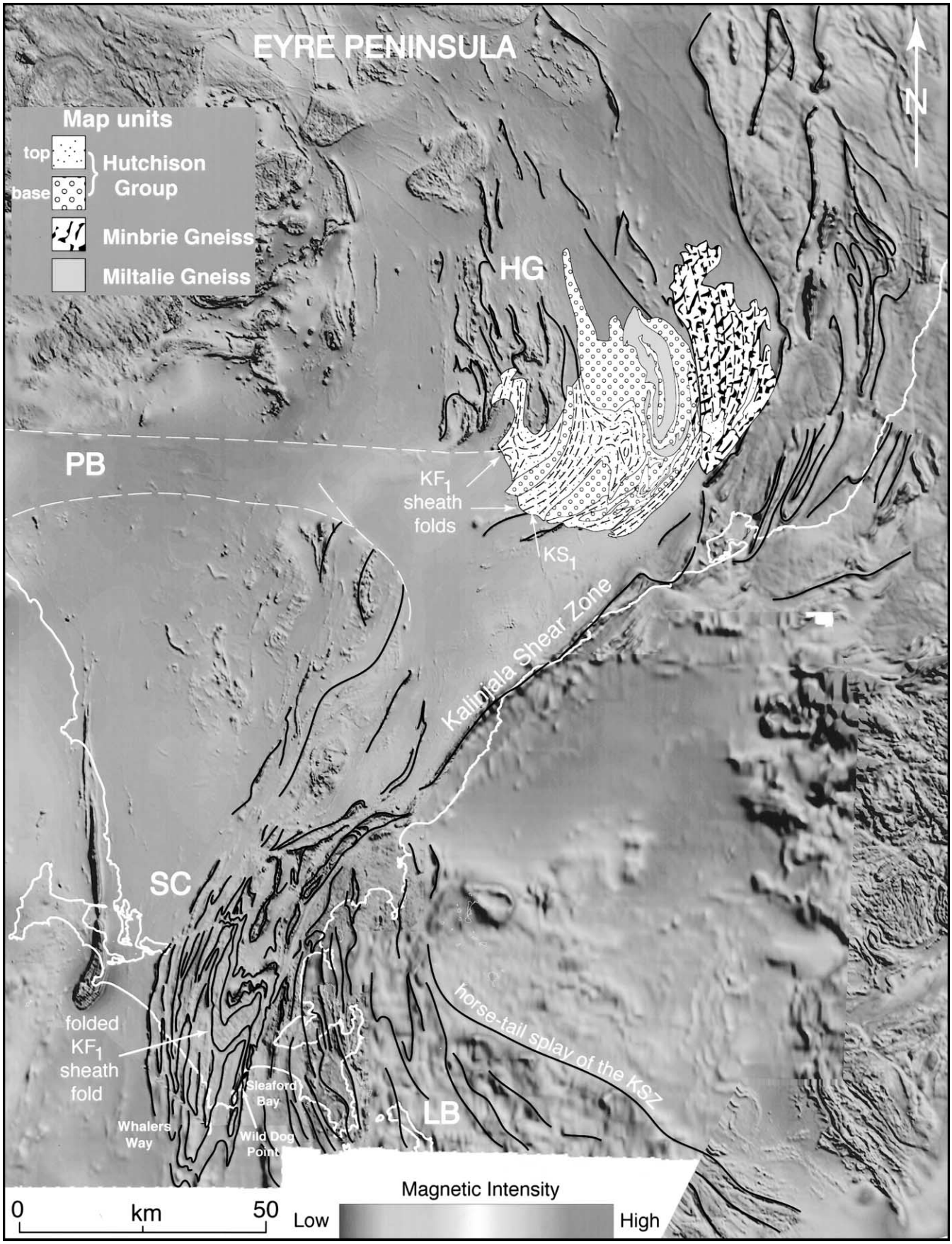
EYRE PENINSULA
N
Map units
top
base
Hutchison Group
Minbrie Gneiss
Miltalie Gneiss
HG
PB
KF1 sheath folds
KS1
Kalinjala Shear Zone
SC
folded KF1 sheath fold
horse-tail splay of the KSZ
Sleaford Bay
Whalers Way
Wild Dog Point
LB
0
km
50
Low
Magnetic Intensity
High

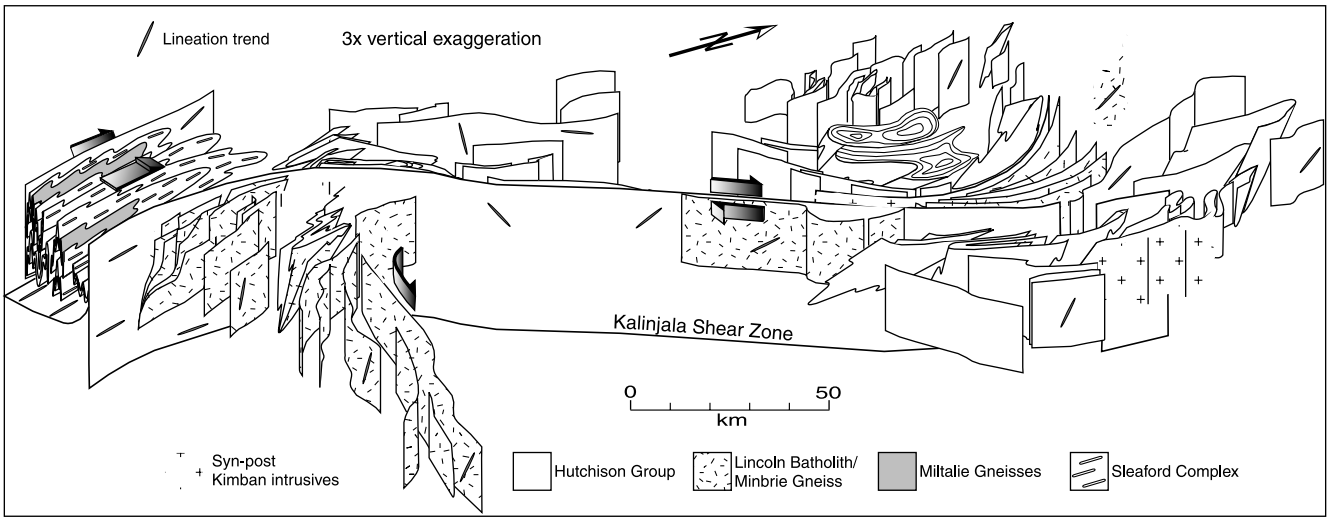

Fig. 16. Three dimensional depiction of the major shear structures in eastern Eyre Peninsula. All structures are centred on the Kalinjala Shear Zone and secondary shears splaying off it form a 'horse-tail splay' termination array in the Lincoln Batholith. Deformation partitioning into dip–slip and strike–slip zones is suggested by the sub-horizontal lineations at Whalers Way and the steep lineations in the Lincoln Batholith.

motion suggests that material flow has been more complex than that of a monoclinic shear system.

6. The importance of identifying the products of non-coaxial deformation

The Eyre Peninsula preserves good indicators of the products of a regional scale non-coaxial deformation such as highly non-cylindrical folds developed under high-grade metamorphic conditions. However, identifying these structures is difficult in many areas due to the overprinting of younger structures (in this case during the same orogenic event) and is further hampered by limited outcrop and/or extensive cover sequences.

In the case where initially flat-lying sheath folds are dissected by later shear zones and become fully dismembered, the initial fold geometry may be completely reoriented. This may lead to incorrect interpretations of transport direction, where movement on the shears is apparently perpendicular to that of the true direction of rock movement during KD_1 (Lacassin and Mattauer, 1985). This is especially true when a number of recent articles reporting variable transport directions with respect to elongation lineation long axes is considered (Passchier, 1997; Tikoff and Greene, 1997; Lin et al., 1997). Non-coaxial deformation processes should be considered in high-grade terrains containing: (1) widespread layer-parallel fabrics (especially where mylonitic and no, or apparently rare, accompanying folds are observed); (2) abundant highly prolate linear clasts; (3) both apparent Type 2 and Type 3 interference patterns (Ramsay and Huber, 1983) and a lineation sub-perpendicular to the fold hinge lines. Caution is therefore needed before attributing deformation to sub-horizontal flattening (coaxial deformation) rather than transpositional shearing in large shear zones. In high-grade rocks non-coaxial deformation effects are not easily identifiable as several subsequent deformation events may dismember sheath folds beyond recognition. Interpreting rocks that have been deformed by non-coaxial processes as having been deformed by coaxial deformations may easily lead to incorrect interpretations of the transport direction.

7. Conclusions

Structures preserved in reworked Archaean to Proterozoic granulites of Eyre Peninsula indicate that the highest strain tectonic event, the ~1730–1700 Ma Kimban Orogeny, formed as a result of the progressive development of the Kalinjala Shear Zone. The first event (KD_1) produced numerous sheath folds during a dextral top-to-the-north shearing event synchronous with north–south stretching. A period of east–west flattening (KD_2) followed the first event. KD_2 localised strain to form hinterland-dipping

Fig. 15. Regional aeromagnetic picture of the Eyre Peninsula. Interpretation of regional strain distribution based on aeromagnetic intensities. Along the southern coast strain increases to the west from Jussieu Peninsula to Whalers Way in accordance with the variation in clast shapes in Fig. 13. Strain is focussed along the Spencer Gulf coast in the thinner central portions of the Kalinjala Shear Zone. The Jussieu Peninsula lies in 'horse-tail splay' of the Kalinjala Shear Zone indicated by the variation of strain in the part of the belt and the rotation of smaller shear zones (the size of individual headlands) into the central zone. A map of the Hutchison Group metasediments is overlain in the central Eyre Peninsula to highlight the structures in the large area of low magnetic intensity. LB = Lincoln Batholith. HG = Hutchison Group. SC = Sleaford Complex. PB = Polda Basin (Phanerozoic).

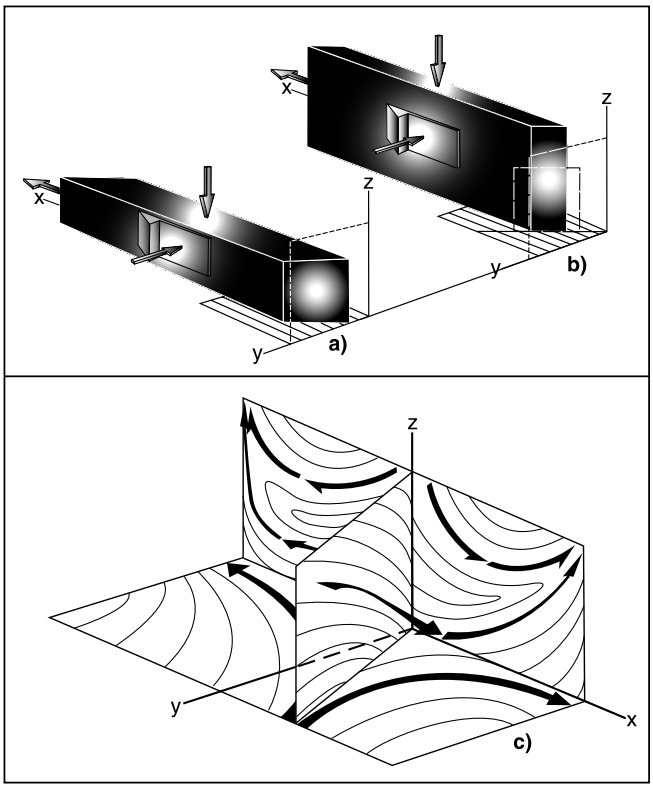

Fig. 17. Diagrams depicting the two states of transpression and idealised particle flow paths recorded by rocks during the Kimban Orogeny assuming monoclinic flow. (a) A large component of sub-horizontal stretching developed prolate 'constrictional' structures during regional dextral shear, elongating the belt in a north–south direction. (b) A following period of east–west sub-horizontal flattening transported the rocks from the margins towards the centre of the Kalinjala Shear Zone. (c) Idealised particle flow paths for rocks in the belt that suffered equal proportions of the two different strain events. After Fossen and Tikoff (1998).

duplex and positive flower structures (Fig. 9) synchronous with the development of tight chevron folds. Kimban deformation is characterised as a dextral transpressional event that may be classified as type E during the first deformation and type C transpression during the second when considered in a monoclinic deformation regime (Fossen and Tikoff, 1998). However, stretching lineation plunge variances of the across the belt suggest the Kalinjala Shear Zone is triclinic.

Semi-quantitative measures of strain across the belt were achieved by the application of four different strain measurement techniques. Measurements completed in rocks with *X/Z* ratios >12 result in increasing inaccuracies and larger assumptions. In particular, as volume loss $-\Delta_A$ due to generation of melt, or gains $+\Delta_A$ as a function of retrogression, have not been constrained, so only *X/Z* ratios could be reported here. Nevertheless, the applied techniques provide a first numerical estimate of the strain preserved in a transitional granulite facies shear belt. Fry analyses were most useful in determining the *X/Z* ratios in weakly deformed areas containing stretches of <7. Deformed enclave dimensions recorded *X/Z* ratios of up to 10. Measurements of individual deformed clast (and rare initially sub-spherical leucosomes in mafic dykes) dimensions suggest that maximum *X/Z* ratios reached up to 25. Clast measurements in areas of variable KD_2 structural development suggest a highly constrictional primarily *L*-fabric was overprinted by subsequent flattening strains. Strain was commonly localised into the highly magnetically susceptible, but initially mechanically weaker, mafic dykes allowing the use of geophysical methods in conjunction with structural observations to define a series of southerly-plunging antiformal and synformal refolded nappes along the margins of the Kalinjala Shear Zone.

Caution must be heeded when dealing with terrains containing a very intense early layer-parallel fabric. This is especially the case where a strong linear fabric is overprinted by later shear zones, or an upright set of tight folds, as it is likely to indicate the presence of a series of dismembered sheath folds. The lack of recognition of sheath folds may possibly lead to an incorrect interpretation of the true tectonic transport direction.

Acknowledgements

John Parker and Mark Fanning are thanked for introducing us to the problems of the Eyre Peninsula. Sue Daly

and Michael Schwarz from Primary Industries and Resources, South Australia, are thanked for their discussions of the Eyre Peninsula geology and their support of the project. We are particularly indebted to Hans Hoek for our numerous discussions concerning the role of contrasting rock rheologies in localising strain. The participants of the SGTSG field trip in February 1999 are also thanked for their provocative discussions. We also thank Dick Norris and an anonymous reviewer for thorough reviews that improved the quality of this paper. Financial support from Australian Research Grant A39533031 is gratefully acknowledged and JJV acknowledges the support of an Australian Postgraduate Research Award.

References

Alsop, G.I., Holdsworth, R.E., 1999. Vergence and facing patterns in large-scale sheath folds. Journal of Structural Geology 21, 1335–1349.

Bales, T., 1996. A structural analysis of Wanna, South Australia: The comparative behaviour of mafic dykes and granite during deformation. B.Sc. (Hons) Thesis, The University of Melbourne.

Brown, M., 1998. Unpairing metamorphic belts: P–T paths and a tectonic model for the Ryoke Belt, southwest Japan. Journal of Metamorphic Geology 16, 3–22.

Cladouhos, T.T., Allmendinger, R.W., 1993. Finite strain and rotation from fault-slip data. Journal of Structural Geology 15, 771–784.

Cobbold, P.R., Quinquis, H., 1980. Development of sheath folds in shear regimes. Journal of Structural Geology 2, 119–126.

Creaser, R.A., Fanning, C.M., 1993. A U–Pb zircon study of the Mesoproterozoic Charleston Granite, Gawler Craton, South Australia. Australian Journal of Earth Sciences 40, 519–526.

Drexel, J.F., Preiss, W.V., Parker, A.J. (Eds.), 1993. The geology of South Australia: Volume 1. The Precambrian. Geological Survey of South Australia Bulletin 54.

Fanning, C.M., 1997. Geochronological synthesis of southern Australia, Part II, The Gawler Craton, South Australia. Department of Mines and Energy. Open file envelope 8918.

Fanning, C.M., Aleinikoff, J.N., 1998. Complex zoning in monazite as revealed by backscatter imaging and SHRIMP analysis. Geological Society of America, Abstract, 51649.

Fanning, C.M., Oliver, R.L., Cooper, J.A., 1980a. The Carnot Gneisses, southern Eyre Peninsula. Quarterly Geological Notes, Geological Survey of South Australia 80, 7–12.

Fanning, C.M., Oliver, R.L., Cooper, J.A., 1980b. The Carnot Gneisses, a metamorphosed Archaean supracrustal sequence in southern Eyre Peninsula. Journal of the Geological Society of Australia, Abstracts 27, 47.

Fanning, C.M., Flint, R.B., Parker, A.J., Ludwig, K.R., Blisset, A.H., 1988. Refined Proterozoic evolution of the Gawler Craton, South Australia, through U–Pb Zircon geochronology. Precambrian Research 40/41, 363–386.

Fossen, H., Tikoff, B., 1998. Extended models of transpression and transtension, and application to tectonic settings. In: Holdsworth, R.E., Strachan, R.A., Dewey, J.F. (Eds.), Continental Transpressional and Transtensional Tectonics. Geological Society, London, Special Publications 135, pp. 15–33.

Foster, D.A., Ehlers, K., 1998. 40Ar–39Ar thermochronology of the southern Gawler Craton, Australia: Implications for Mesoproterozoic and Neoproterozoic tectonics of East Gondwana and Rodinia. Journal of Geophysical Research 103, 10177–10193.

Fry, N., 1979. Random point distributions and strain measurement in rocks. Tectonophysics 60, 89–105.

Ghosh, S.K., 1993. Structural Geology—Fundamentals and Modern Developments. Pergamon Press, Oxford.

Goscombe, B., Passchier, C., 2001. Boudin trains as a kinematic tool. Specialist Group in Tectonics and Structural Geology, Geological Society of Australia, Abstracts 64, 63–64.

Hand, M., Bendall, B.R., Sandiford, M., 1995. Metamorphic evidence for Palaeoproterozoic oblique convergence in the eastern Gawler Craton. Geological Society of Australia, Abstracts 40, 59.

Hoek, J.D., Schaefer, B.F., 1998. The Palaeoproterozoic Kimban mobile belt, Eyre Peninsula: Timing and significance of felsic and mafic magmatism and deformation. Australian Journal of Earth Sciences 45, 305–313.

Jezek, J., Schulmann, K., Segeth, K., 1996. Fabric evolution of rigid inclusions during mixed coaxial and simple shear flows. Tectonophysics 257, 203–221.

Jiang, D., Williams, P.F., 1998. High-strain zones: a unified model. Journal of Structural Geology 20, 1105–1120.

Lacassin, R., Mattauer, M., 1985. Kilometre-scale sheath fold at Mattmark and implications for the transport direction in the Alps. Nature 315, 739–741.

Lin, S., Jiang, D., Williams, P.F., 1997. Transpression (or transtension) zones of triclinic symmetry: natural example and theoretical modelling. In: Holdsworth R.E., Strachan, R.A., Dewey, J.F. (Eds.), Continental Transpressional and Transtensional Tectonics. Geological Society, London, Special Publications 135, pp. 15–33.

Miller, E.-L.G., 1999. A structural analysis and strain distribution of the Wild Dog Point region, Eyre Peninsula, South Australia. B.Sc. (Hons) Thesis, The University of Melbourne.

Mortimer, G.E., Cooper, J.A., Oliver, R.L., 1988. The geochemical evolution of Proterozoic granitoids near Port Lincoln in the Gawler orogenic domain of South Australia. Precambrian Research 40/41, 387–406.

Parker, A.J., 1980. The Kalinjala Mylonite Zone, eastern Eyre Peninsula. Quarterly Geological Notes, Geological Survey of South Australia 76, 6–11.

Parker, A.J., 1993. Kimban Orogeny. In: Drexel, J.F., Preiss, W.V., Parker, A.J. (Eds.), The Geology of South Australia: Volume 1, The Precambrian. Geological Survey of South Australia Bulletin 54.

Parker, A.J., Lemon, N.M., 1982. Reconstruction of the Early Proterozoic stratigraphy of the Gawler Craton, South Australia. Journal of the Geological Society of Australia 29, 221–238.

Parker, A.J., Rickwood P.C., Baillie, P.W., Boyd, D.M., McClenaghan, M.P., Freeman, M.J., Pietsch, B.A., Murray, C.G., Myers, J.S., 1987. Mafic dyke swarms of Australia. In: Halls, H.C., Fahrig, W.F. (Eds.), Mafic Dyke Swarms; a Collection of Papers Based on the Proceedings of an International Conference. Special Paper—Geological Association of Canada 34, pp. 401–417.

Parker, A.J., Fanning, C.M., Flint, R.B., Martin, A.R., Rankin, L.R., 1988. Archaean–Early Proterozoic granitoids, metasediments and mylonites of southern Eyre Peninsula, South Australia. Specialist Group in Tectonics and Structural Geology Field Guide Series No. 2. Geological Society of Australia.

Passchier, C.W., 1997. The fabric attractor. Journal of Structural Geology 19, 113–127.

Pollard, D.D., Segall, P., Delaney, P.T., 1982. Formation and interpretation of dilatant echelon cracks. Geological Society of America Bulletin 93, 1291–1303.

Ramsay, J.G., Huber, M.I., 1983. The Techniques of Modern Structural Geology. Strain Analysis, vol. 1. Academic Press, London.

Rankin, L.R., Flint, R.B., Fanning, C.M., 1988. The Bosanquet Formation of the Gawler Craton. South Australian Geological Survey. Quarterly Geological Notes 105, 12–18.

Schaefer, B., 1998. Insights into Proterozoic tectonics from the southern Eyre Peninsula, South Australia. Ph.D. Thesis, The University of Adelaide.

Schwarz, M., 1999. Definition of the Moody Suite, southern Gawler Craton. MESA Journal April, 39–44.

Schulmann, K., Mlcoch, B., Melka, R., 1996. High-temperature

microstructures and rheology of deformed granite, Erzgebirge, Bohemian Massif. Journal of Structural Geology 18, 719–733.

Sengupta, S., 1997. Contrasting fabrics in deformed dykes and host rocks: natural examples and a simplified model. In: Sengupta, S. (Ed.), Evolution of Geological Structures from Micro- to Macroscales. Chapman and Hall, London, pp. 303–319.

Skjernaa, L., 1989. Tubular folds and sheath folds: definitions and conceptual models for their development, with examples from the Grapevare area, northern Sweden. Journal of Structural Geology 11, 689–703.

Tikoff, B., Greene, D., 1997. Stretching lineations in transpressional shear zones: an example from the Sierra Nevada Batholith. California. Journal of Structural Geology 19, 29–39.

Thomson, B.P. (Compiler), 1980. Geological map of South Australia. South Australia, Geological Survey. Maps of South Australia Series, 1:1,000,000.

Turner, S., Foden, J., Sandiford, M., Bruce, D., 1993. Sm–Nd evidence for the provenance of sediments from the Adelaide Fold Belt and southeastern Australia with implications for episodic crustal addition. Geochimica et Cosmochima Acta 57, 1837–1856.

Vassallo, J.J., Wilson, C.J.L., 1999a. A structural reinterpretation of the southern Eyre Peninsula, South Australia. Specialist Group in Tectonics and Structural Geology, Geological Society of Australia, Abstracts 53, 265–266.

Vassallo, J.J., Wilson, C.J.L., 1999. Palaeoproterozoic geology of southeastern Eyre Peninsula, South Australia. In: Wilson, C.J.L. (Ed.), The Great Southern Transect II: a geological section incorporating the Lachlan Fold Belt, Adelaide Fold Belt and Gawler Craton, Halls Gap (Victoria) to Port Lincoln (SA). Specialist Group in Tectonics and Structural Geology, Field Guide 6, Geological Society of Australia.

Vassallo, J.J., Wilson, C.J.L., 2001. Structural repetition of the Hutchison Group metasediments, Eyre Peninsula, South Australia. Australian Journal of Earth Sciences 48, 332–346.

Webb, A.W., Thomson, B.P., Blissett, A.H., Daly, S.J., Flint, R.B., Parker, A.J., 1986. Geochronology of the Gawler Craton, South Australia. Australian Journal of Earth Sciences 33, 119–143.

Windley, B.F., 1993. Uniformitarianism today: the present is the key to the past. Journal of the Geological Society of London 15, 7–19.